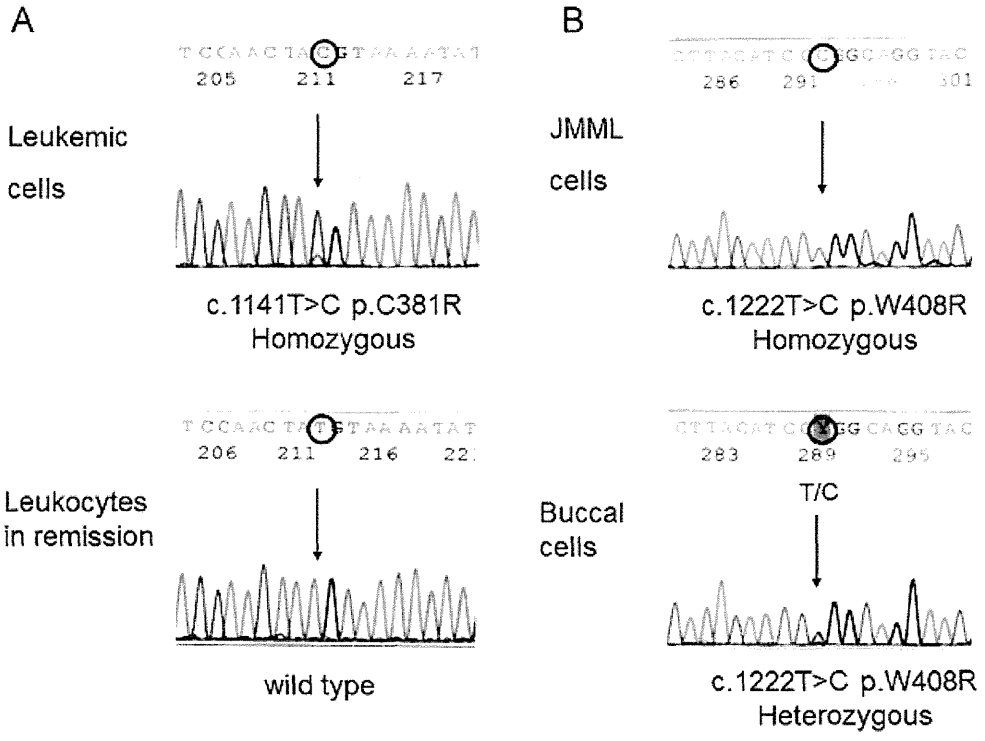

Fig. 1. *CBL* mutations identified in patients. (A) Sequencing charts of leukemic cells and peripheral blood at complete remission from Patient PL1. (B) Sequencing charts of JMML cells and buccal mucosa from Patient PL52.

CBL mutations are associated with an 11q-acquired uniparental disomy (aUPD) involving the *CBL* locus, which converts these mutations into a homozygous state [3]. An SNP array analyzed the difference in DNA between PB samples at disease onset (leukemia cells) and leukocytes in remission. The analysis revealed a UPD 11q13.1qter that contained the *CBL* locus only in the T-ALL sample (Table 1). In addition, homozygous deletions of 4q25, which encodes the *LEF1* gene, and of 9p21.3, including the region that encodes *CDKN2A*, were detected. A UPD at 9pter-p13.3 was also observed. The deletion of 14q11.2, which encodes *TCRA*, and the one-copy deletion in 7q34 (including *TCRB*) that were observed in the DNA from the T-ALL cells may be due to a TCR rearrangement. The effects of the gain of the immunoglobulin light chain at 2p11.2 and the gain at 17q12, which contains *CCL3L3*, *CCL4L2* and *TBC1D3*, are unknown.

3.4. *ELK and c-Jun transactivation in cells expressing mutant CBL proteins*

The *CBL* p.C381R mutation that was identified in one T-ALL patient has also been identified in a JMML patient and a single patient with MDS [5,23]. However, a functional analysis of p.C381R has not been performed.

A WT allele and the two *CBL* mutants, p.C381R and p.R420Q, were introduced in NIH 3T3 cells, and ELK transactivation was examined to elucidate the activation of the ERK pathway. The allele p.R420Q was used as a positive control because this mutant activates ERK [12]. ELK is a transcription factor that is phosphorylated by activated ERK and that binds the serum response element in the promoters of the immediate early genes, including c-FOS [24]. ELK transactivation was remarkably enhanced in cells expressing

Table 1
Genetic abnormalities of T-ALL at diagnosis.

Chromosomal sites	Copy number state (leukemia)	Copy number state (germline)	Loss/gain	Size (kb)	*Start_Linear_Position	*End_Linear_Position	Genes included in the region
11q13.1qter		2	UPD	69575.00	64877380	134452384	*CBL* and others
14q11.2	1	2	Loss	369.94	21660717	22030660	*TCRA, TCRD, TCR*
17q12	3	2	Gain	192.98	31460821	31653797	*CCL3L3, CCL4L2, TBC1D3*
2p11.2	4	3	Gain	460.63	88914227	89374858	*IGK@*
2p11.2	3	2	Gain	109.16	89753412	89862571	*IGK@*
4q25	0	2	Loss	104.82	109199454	109304271	*LEF1*
7q34	0	2	Loss	491.97	141711730	142203700	*TCRB*
9p11.2	3	2	Gain	127.88	44667843	44795721	
9p21.3	0	2	Loss	117.67	21864256	21981923	*CDKN2A*
9pterp13.3		2	UPD	33701.54	1	33701540	*CDKN2A* and others

Abbreviations: CBL, Cas-Br-M (murine) ecotropic retroviral transforming sequence; TCRA, T cell receptor alpha; TCRD, T cell receptor delta; CCL3L3, chemokine ligand 3-like 3; CCL4L2, chemokine ligand 4-like 2; TBC1D3, TBC1 domain family, member 3; IGK@, immunoglobulin kappa locus; LEF1, lymphoid enhancer binding factor 1; TCRB, T cell receptor beta; CDKN2A, cyclin-dependent kinase inhibitor 2A.

* Denoted by NCBI 36 reference human genome (hg18).

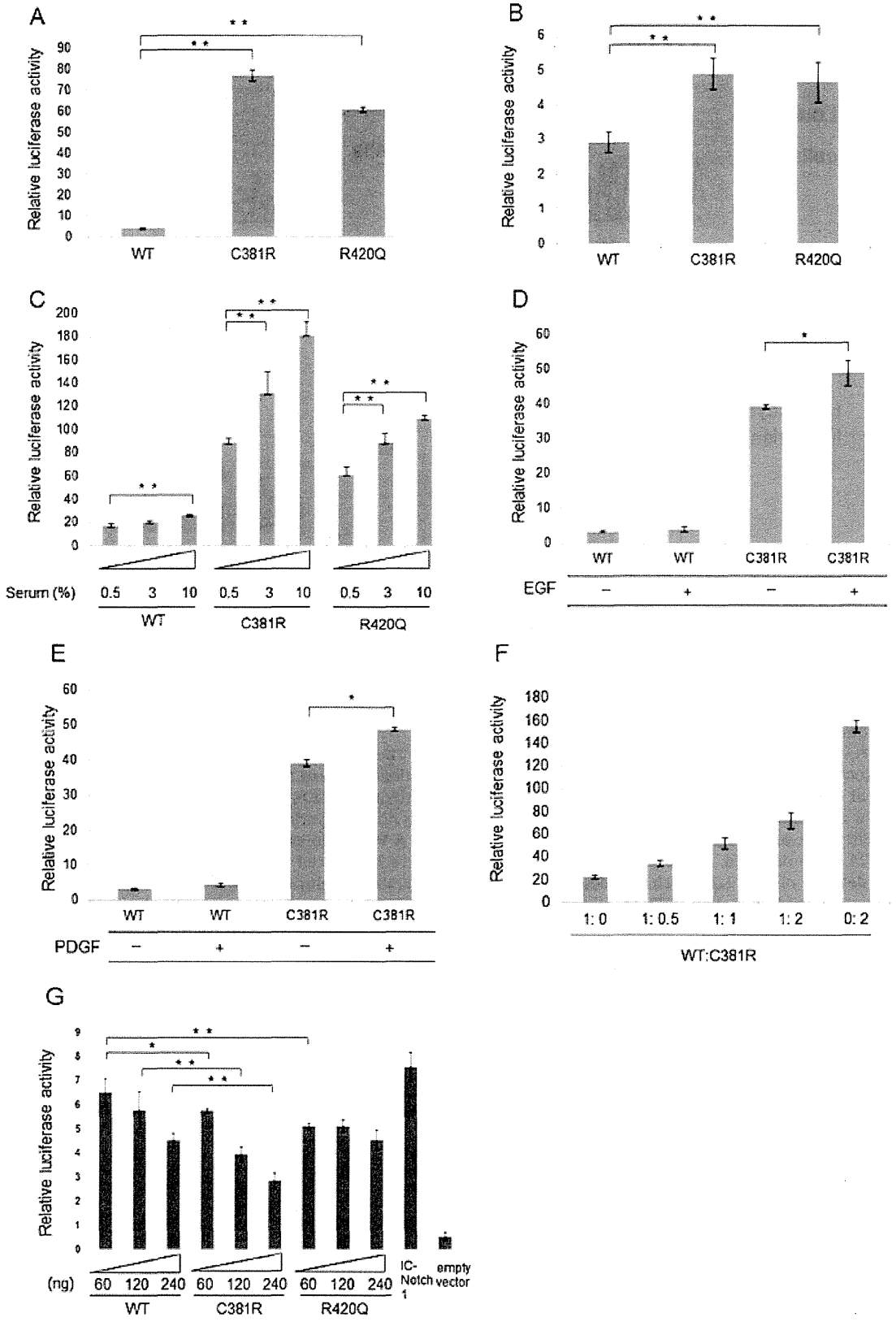

Fig. 2. ELK, c-Jun, and HES1 transactivation in cells expressing mutant CBL proteins. The results are expressed as the mean and standard deviation of mean values from triplicate samples. $^{**}P<0.01$ and $^{*}P<0.05$ determined with Student's t-test. (A) ELK transactivation in cells with WT CBL and mutant CBL. (B) c-Jun transactivation in cells with WT CBL and mutant CBL. (C) ELK transactivation in NIH 3T3 cells transiently expressing WT CBL and C381R CBL in DMEM that contained the indicated concentrations of newborn calf serum (NCS). (D) For EGF stimulation, the ELK transactivation level in cells expressing p.C381R stimulated with EGF was significantly enhanced compared

p.C381R and p.R420Q in DMEM containing 10% NCS compared with WT *CBL*-transfected cells (Fig. 2A). The transactivation of the transcription factor c-Jun was examined in NIH 3T3 cells. Studies have shown that c-Jun activity is upregulated by the phosphorylation of c-Jun NH2-terminal kinases (JNK) [25]. In this case, c-Jun transactivation was significantly enhanced in cells expressing p.C381R and p.R420Q in DMEM containing 10% NCS (Fig. 2B). These results demonstrate that *CBL* mutants activate the ERK and JNK pathways, possibly via the upstream activation of RAS in the presence of serum.

ELK transactivation was examined in different NCS concentrations to evaluate the effect of serum concentration. ELK transactivation in cells expressing p.C381R and p.R420Q was enhanced in an NCS concentration-dependent manner (Fig. 2C). Significant ELK activation was observed in cells expressing p.C381R and p.R420Q in DMEM with 0.5% NCS. The effects of EGF and PDGF on ELK transactivation were examined in cells expressing WT *CBL* or p.C381R *CBL*. The ELK transactivation levels in cells expressing p.C381R that were stimulated with 100 ng/ml EGF (Fig. 2D) or 100 ng/ml PDGF (Fig. 2E) were significantly enhanced compared with those of unstimulated cells. However, EGF and PDGF stimulation did not significantly alter the ELK transactivation levels in cells expressing WT *CBL*. These results suggest that the p.C381R mutation constitutively activates the RAS pathway.

CBL mutations affect endogenous WT CBL in a dominant-negative manner [7]. NIH 3T3 cells were co-transfected with WT CBL and C381R to evaluate the effect of p.C381R on WT CBL. The hypertransactivation response that was induced by the CBL mutant was abolished by the co-transfection of WT CBL (Fig. 2F), suggesting the pathogenic importance of the WT *CBL* allele loss.

3.5. *HES transactivation in cells expressing mutant CBL*

HES1 is a target gene for NOTCH1. WT or mutant CBL constructs were transiently transfected in NIH 3T3 cells with the HES-Luc reporter and a constitutively active intracellular domain of NOTCH1 (ICN1) construct. ICN1 expression significantly increased the transactivation of HES (Fig. 2G, IC-NOTCH1 lane). The introduction of CBL WT or mutants significantly reduced the HES transactivation levels compared with cells expressing ICN1 (Fig. 2G). The HES1 transactivation levels in cells expressing p.C381R were significantly decreased compared with CBL WT-expressing cells.

4. Discussion

In this study, a homozygous p.C381R mutation and a UPD of the region that included *CBL* were identified in T-ALL cells, and a heterozygous germline p.W408R mutation was identified in one patient with JMML. An additional mutation analysis identified two *NOTCH1* mutations and homozygous deletions of *LEF1* and *CDKN2A* in T-ALL cells. A functional analysis revealed that cells expressing the p.C381R mutant constitutively transactivated ELK and c-Jun. Co-transfection of WT and the p.C381R mutation in NIH 3T3 cells revealed that WT inhibited the ELK-activating effects of p.C381R. The HES1 transactivation levels in cells expressing p.C381R were significantly decreased compared with CBL WT-expressing cells, suggesting that this *CBL* mutation plays a role in NOTCH signaling pathway.

CBL mutations are rare in ALL patients. Recently, mutations in *CBL* have been identified in 2 infant ALL patients with *MLL* gene rearrangements [26]. Nicholson et al. analyzed the linker-RING domains of CBL in a cohort of 180 diagnostic and 46 relapsed ALL patients and identified deletions/insertions of *CBL*, including the splicing acceptor or donor site of exon 8 in three ALL samples [27]. *CBL* mutations in ALL may promote the proliferation of leukemia cells by activating the RAS pathway ([27] and our study). Alternatively, our HES-reporter assay in cells that expressed the *NOTCH1* constitutive active mutant showed that *CBL* p.C381R downregulated the NOTCH1 signaling pathway, suggesting that the *CBL* p.C381R mutation may contribute to leukemogenesis through interaction with NOTCH1. The relationship between CBL and NOTCH1 has not been elucidated, but one report has demonstrated that CBL promotes the ubiquitin-dependent lysosomal degradation of membrane-associated NOTCH1 [28]. In the case of NOTCH3, its interactions with pre-TCR lead to the recruitment and persistence of the CBL to the lipid rafts in thymocytes from mice expressing the constitutively active intracellular domain of NOTCH3, which suggests that CBL may regulate the NOTCH3 and pre-TCR relationship during T-cell leukemogenesis [29]. Further analysis will elucidate the role of the *CBL* mutation in T-ALL leukemogenesis.

Somatic and germline *CBL* mutations have been clustered in either the linker domain or the RING finger domain (Fig. 3). The loss of the ubiquitination of activated receptor tyrosine kinases is thought to contribute to the transforming potential of leukemia-associated mutant CBL proteins. The distributions of somatic and germline mutations were almost similar. However, Y371, which is a hot spot for *CBL* mutations in JMML, is rarely mutated in other myeloid malignancies [5]. The germline p.W408R mutation has been identified in a patient with JMML [5]. Individuals with germline *CBL* mutations display a variable combination of dysmorphic features, including mild hypertelorism, a short upturned nose, a deeply grooved philtrums and thick lips, which are reminiscent of the facial gestalt of NS [10]. Patient PL52, who had a germline p.W408R mutation, had normal development and no dysmorphic features at 15 months of age. However, her young age may have precluded any firm conclusions. Long-term follow-up examinations and an analysis of wider cohorts is necessary to further characterize the phenotypic spectrum that is associated with germline mutations in *CBL*.

The effect of mutant CBLs on ERK activation depends on the level of endogenous WT CBL [7,30]. Therefore, we examined ELK transactivation in NIH 3T3 cells, which have low endogenous CBL protein expression [31]. Our study demonstrated that ELK transactivation in cells expressing p.C381R decreased with increasing WT CBL expression. These results suggest that the p.C381R mutation functions in a dominant-negative manner or as a gain-of-function mutation.

In this study, SNP array analyses of samples from leukemia cells and leukocytes obtained from patients in remission revealed a copy number imbalance that was specific for leukemia cells. The homozygous deletion of the entire *LEF1* gene was identified in the T-ALL sample with the *CBL* mutation. LEF1 is a member of the lymphoid enhancer factor/T-cell factor family of DNA-binding transcription factors that interact with nuclear β-catenin in the WNT signaling pathway [32]. Monoallelic or biallelic *LEF1* microdeletions have been identified in 11% (5 of 47) of primary samples from the diagnostic specimens of 47 children with T-ALL, using high-resolution array comparative genomic hybridization [33]. The homozygous deletion of *CDKN2A* and

with unstimulated cells. (E) For PDGF stimulation, the ELK transactivation level in cells expressing p.C381R stimulated with 100 ng/ml PDGF was enhanced compared with unstimulated cells. (F) Co-transfection of WT CBL and C381R CBL. The hypertransactivation response induced by CBL p.C381R was abolished by the co-transfection of WT CBL. (G) Mutant CBL constructs in pCMV6 were transiently transfected in NIH 3T3 cells with the HES-Luc reporter and the intracellular NOTCH1 (ICN1) construct where appropriate.

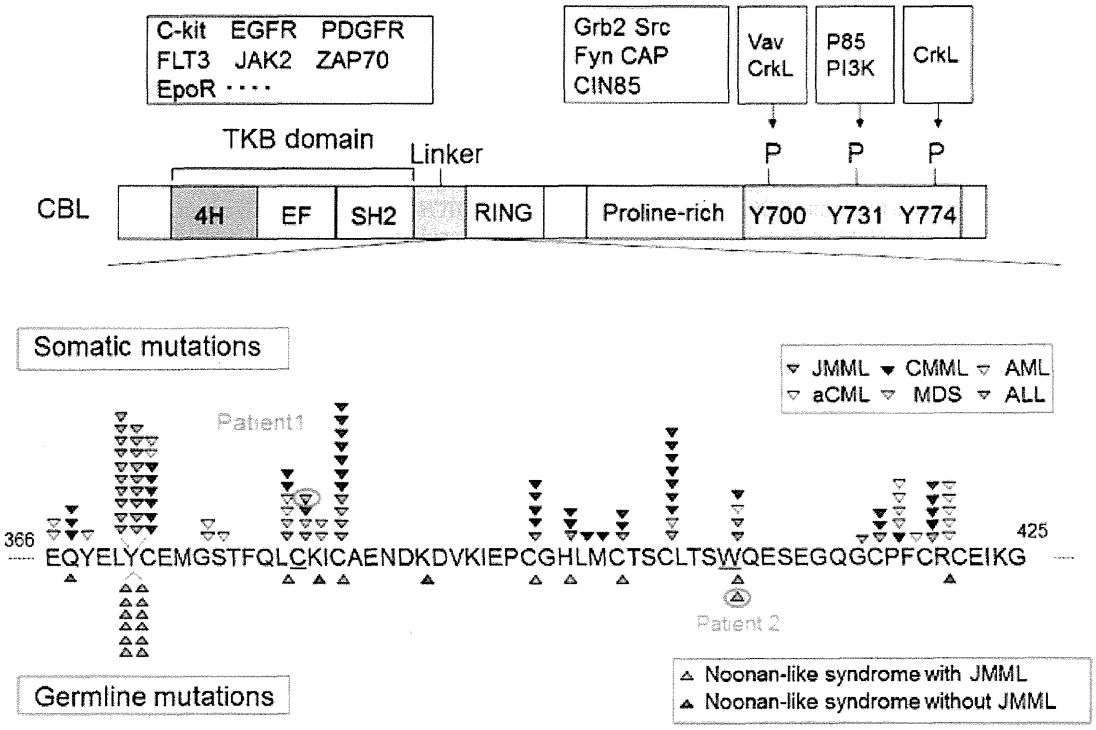

Fig. 3. The CBL structure and mutation spectrum. CBL comprises an N-terminal tyrosine kinase binding domain (TKB) connected by a linker to the RING-finger domain implicated in E2 enzyme binding. These domains are followed by a proline-rich region and a C-terminal portion containing tyrosine phosphorylation sites. The molecular interaction of CBL with cytokine receptors and other signaling molecules are also shown on top. The *CBL* mutations identified in hematologic malignancies partially overlap with those identified in the germline.

CDKN2B, which are frequently inactivated in various hematological malignancies [34], was also identified in the T-ALL sample. A comparison of the copy numbers of DNA samples from leukemia cells and germline DNA will help to highlight the abnormalities in leukemia.

In conclusion, we identified a *CBL* p.C381R mutation in leukemia cells from one patient with T-ALL. A functional analysis demonstrated that the mutation constitutively activated the RAS-MAPK pathway and inhibited the constitutive activation of the NOTCH signaling pathway. Further studies will be needed to determine the relationship between CBL and leukemogenesis.

Conflict of interest statement

All authors declare no competing financial interests.

Acknowledgments

The authors thank the patients, their families and the doctors who participated in this study. We are grateful to Dr. Tasuku Honjo at Kyoto University for supplying the HES-Luc expression construct in pGV-B and mouse intracellular NOTCH1 region expression construct in pEF-BOSneo. We are also grateful to Drs. Kunihiko Moriya and Naoto Ishii for their helpful discussions. We thank Kumi Kato, Yoko Tateda and Riyo Takahashi for their technical assistance. This work was supported by the Funding Program for the Next Generation of World-Leading Researchers (NEXT Program) from the Ministry of Education, Culture, Sports, Science and Technology of Japan to YA and from the Ministry of Health, Labor and Welfare to YM and YA. This work was supported in part by the National Cancer Center Research and Development FUND (23-22-11).

Contributions. YS, YA and SK designed the research study; YS, HM, HM and TN performed the research; MI, TR, YS, ST and SK provided patients samples; YS, HM, HM and JPM analyzed the data; YS, YA and YM wrote the paper.

Appendix A. Supplementary data

Supplementary data associated with this article can be found, in the online version, at http://dx.doi.org/10.1016/j.leukres.2012.04.018.

References

[1] Langdon WY, Hartley JW, Klinken SP, Ruscetti SK, Morse 3rd HC. v-cbl, an oncogene from a dual-recombinant murine retrovirus that induces early B-lineage lymphomas. Proc Natl Acad Sci USA 1989;86:1168–72.
[2] Schmidt MH, Dikic I. The Cbl interactome and its functions. Nat Rev Mol Cell Biol 2005;6:907–18.
[3] Dunbar AJ, Gondek LP, O'Keefe CL, Makishima H, Rataul MS, Szpurka H, et al. 250K single nucleotide polymorphism array karyotyping identifies acquired uniparental disomy and homozygous mutations, including novel missense substitutions of c-Cbl, in myeloid malignancies. Cancer Res 2008;68:10349–57.
[4] Grand FH, Hidalgo-Curtis CE, Ernst T, Zoi K, Zoi C, McGuire C, et al. Frequent CBL mutations associated with 11q acquired uniparental disomy in myeloproliferative neoplasms. Blood 2009;113:6182–92.
[5] Loh ML, Sakai DS, Flotho C, Kang M, Fliegauf M, Archambeault S, et al. Mutations in CBL occur frequently in juvenile myelomonocytic leukemia. Blood 2009;114:1859–63.
[6] Muramatsu H, Makishima H, Jankowska AM, Cazzolli H, O'Keefe C, Yoshida N, et al. Mutations of an E3 ubiquitin ligase c-Cbl but not TET2 mutations are pathogenic in juvenile myelomonocytic leukemia. Blood 2010;115:1969–75.
[7] Sanada M, Suzuki T, Shih LY, Otsu M, Kato M, Yamazaki S, et al. Gain-of-function of mutated C-CBL tumour suppressor in myeloid neoplasms. Nature 2009;460:904–8.

[8] Caligiuri MA, Briesewitz R, Yu J, Wang L, Wei M, Arnoczky KJ, et al. Novel c-CBL and CBL-b ubiquitin ligase mutations in human acute myeloid leukemia. Blood 2007;110:1022–4.
[9] Sargin B, Choudhary C, Crosetto N, Schmidt MH, Grundler R, Rensinghoff M, et al. Flt3-dependent transformation by inactivating c-Cbl mutations in AML. Blood 2007;110:1004–12.
[10] Perez B, Mechinaud F, Galambrun C, Ben Romdhane N, Isidor B, Philip N, et al. Germline mutations of the CBL gene define a new genetic syndrome with predisposition to juvenile myelomonocytic leukaemia. J Med Genet 2010;47:686–91.
[11] Niemeyer CM, Kang MW, Shin DH, Furlan I, Erlacher M, Bunin NJ, et al. Germline CBL mutations cause developmental abnormalities and predispose to juvenile myelomonocytic leukemia. Nat Genet 2010;42:794–800.
[12] Martinelli S, De Luca A, Stellacci E, Rossi C, Checquolo S, Lepri F, et al. Heterozygous germline mutations in the CBL tumor-suppressor gene cause a Noonan syndrome-like phenotype. Am J Hum Genet 2010;87:250–7.
[13] Aoki Y, Niihori T, Narumi Y, Kure S, Matsubara Y. The RAS/MAPK syndromes: novel roles of the RAS pathway in human genetic disorders. Hum Mutat 2008;29:992–1006.
[14] Tidyman WE, Rauen KA. The RASopathies: developmental syndromes of Ras/MAPK pathway dysregulation. Curr Opin Genet Dev 2009;19:230–6.
[15] Gondek LP, Tiu R, Haddad AS, O'Keefe CL, Sekeres MA, Theil KS, et al. Single nucleotide polymorphism arrays complement metaphase cytogenetics in detection of new chromosomal lesions in MDS. Leukemia 2007;21:2058–61.
[16] Kurooka H, Kuroda K, Honjo T. Roles of the ankyrin repeats and C-terminal region of the mouse notch1 intracellular region. Nucleic Acids Res 1998;26:5448–55.
[17] Kato H, Sakai T, Tamura K, Minoguchi S, Shirayoshi Y, Hamada Y, et al. Functional conservation of mouse Notch receptor family members. FEBS Lett 1996;395:221–4.
[18] Komatsuzaki S, Aoki Y, Niihori T, Okamoto N, Hennekam RC, Hopman S, et al. Mutation analysis of the SHOC2 gene in Noonan-like syndrome and in hematologic malignancies. J Hum Genet 2010;55:801–9.
[19] Weng AP, Ferrando AA, Lee W, Morris JP, Silverman LB, Sanchez-Irizarry C, et al. Activating mutations of NOTCH1 in human T cell acute lymphoblastic leukemia. Science 2004;306:269–71.
[20] O'Neil J, Grim J, Strack P, Rao S, Tibbitts D, Winter C, et al. FBW7 mutations in leukemic cells mediate NOTCH pathway activation and resistance to gamma-secretase inhibitors. J Exp Med 2007;204:1813–24.
[21] Thompson BJ, Jankovic V, Gao J, Buonamici S, Vest A, Lee JM, et al. Control of hematopoietic stem cell quiescence by the E3 ubiquitin ligase Fbw7. J Exp Med 2008;205:1395–408.
[22] Maser RS, Choudhury B, Campbell PJ, Feng B, Wong KK, Protopopov A, et al. Chromosomally unstable mouse tumours have genomic alterations similar to diverse human cancers. Nature 2007;447:966–71.
[23] Rocquain J, Carbuccia N, Trouplin V, Raynaud S, Murati A, Nezri M, et al. Combined mutations of ASXL1, CBL, FLT3, IDH1, IDH2, JAK2, KRAS, NPM1, NRAS, RUNX1, TET2 and WT1 genes in myelodysplastic syndromes and acute myeloid leukemias. BMC Cancer 2010;10:401.
[24] Gille H, Kortenjann M, Thomae O, Moomaw C, Slaughter C, Cobb MH, et al. ERK phosphorylation potentiates Elk-1-mediated ternary complex formation and transactivation. EMBO J 1995;14:951–62.
[25] Barr RK, Bogoyevitch MA. The c-Jun N-terminal protein kinase family of mitogen-activated protein kinases (JNK MAPKs). Int J Biochem Cell Biol 2001;33:1047–63.
[26] Shiba N, Park MJ, Taki T, Takita J, Hiwatari M, Kanazawa T, et al. CBL mutations in infant acute lymphoblastic leukaemia. Br J Haematol 2012;156:672–4.
[27] Nicholson L, Knight T, Matheson E, Minto L, Case M, Sanichar M, et al. Casitas B lymphoma mutations in childhood acute lymphoblastic leukemia. Genes Chromosomes Cancer 2012;51:250–6.
[28] Jehn BM, Dittert I, Beyer S, von der Mark K, Bielke W. c-Cbl binding and ubiquitin-dependent lysosomal degradation of membrane-associated Notch1. J Biol Chem 2002;277:8033–40.
[29] Checquolo S, Palermo R, Cialfi S, Ferrara G, Oliviero C, Talora C, et al. Differential subcellular localization regulates c-Cbl E3 ligase activity upon Notch3 protein in T-cell leukemia. Oncogene 2010;29:1463–74.
[30] Ogawa S, Shih LY, Suzuki T, Otsu M, Nakauchi H, Koeffler HP, et al. Deregulated intracellular signaling by mutated c-CBL in myeloid neoplasms. Clin Cancer Res 2010;16:3825–31.
[31] Lo FY, Tan YH, Cheng HC, Salgia R, Wang YC. An E3 ubiquitin ligase: c-Cbl: a new therapeutic target of lung cancer. Cancer 2011;117:5344–50.
[32] van Noort M, Clevers H. TCF transcription factors, mediators of Wnt-signaling in development and cancer. Dev Biol 2002;244:1–8.
[33] Gutierrez A, Sanda T, Ma W, Zhang J, Grebliunaite R, Dahlberg S, et al. Inactivation of LEF1 in T-cell acute lymphoblastic leukemia. Blood 2010;115:2845–51.
[34] Ruas M, Peters G. The p16INK4a/CDKN2A tumor suppressor and its relatives. Biochim Biophys Acta 1998;1378:F115–77.

Clinical Endocrinology (2012) 76, 78–87 doi: 10.1111/j.1365-2265.2011.04165.x

ORIGINAL ARTICLE

Identification of a novel mutation in the exon 2 splice donor site of the *POU1F1/PIT-1* gene in Japanese identical twins with mild combined pituitary hormone deficiency

Hiroshi Inoue*·†, Tokuo Mukai‡, Yukiko Sakamoto†, Chizuko Kimura†, Natsumi Kangawa†, Mitsuo Itakura†, Tsutomu Ogata§, Yoshiya Ito‡ and Kenji Fujieda‡ on behalf of the Japan Growth Genome Consortium

*Diabetes Therapeutics and Research Center and †Division of Genetic Information, Institute for Genome Research, The University of Tokushima, Tokushima, ‡Department of Paediatrics, Asahikawa Medical University, Asahikawa and §Department of Endocrinology and Metabolism, National Research Institute for Child Health and Development, Tokyo, Japan

Summary

Context To date, approximately 35 different *POU1F1* mutations have been described in patients with familial and sporadic combined pituitary hormone deficiency (CPHD) from different ethnic backgrounds. The majority are missense mutations clustered within the conserved POU-specific and POU-homeo domains, encoded by exons 4 and 6, respectively.

Objectives This study aimed to identify the molecular basis and clinical characteristics of a Japanese CPHD family with a novel *POU1F1* mutation.

Design The *POU1F1* gene was sequenced in identical twin brothers with mild CPHD. The mutation identified was also evaluated in family members as well as 188 Japanese controls and then examined in functional studies.

Results A novel heterozygous splice site mutation (Ex2 + 1G>T; c.214 + 1G>T) was detected. This mutation was also present in their undiagnosed mother, but not in any of the controls. *In vitro* splicing studies suggested this mutation to result in an in-frame skipping of exon 2, thus producing an internally deleted protein lacking most of the R2 transactivation subdomain (TAD-R2). Heterologous expression studies of the mutated POU1F1 protein showed only modest reductions in its transactivation activities in HEK293T cells, while acting as a dominant-negative inhibitor of the endogenous activities of POU1F1 in pituitary GH3 cells.

Conclusions This is the first report of a mutation at the exon 2 donor splice site of *POU1F1*, affecting TAD-R2. The addition of this mutation to the growing list of pathological *POU1F1* mutations may provide deeper insights into clinical heterogeneity in the expressions of individual mutations and a better understanding of the structure–function relationships of POU1F1.

(Received 12 April 2011; returned for revision 10 May 2011; finally revised 28 June 2011; accepted 29 June 2011)

Correspondence: Hiroshi Inoue, Division of Genetic Information, Institute for Genome Research, The University of Tokushima, Kuramoto 3-18-15, Tokushima 770-8503, Japan. Tel.: +81 88 633 9483; Fax: +81 88 633 9484; E-mail: hinoue@genome.tokushima-u.ac.jp

Present address: T. Mukai, Department of Paediatrics, Asahikawa Kosei General Hospital, Asahikawa, Japan.

Present address: Y. Ito, Department of Basic Sciences, Japanese Red Cross Hokkaido College of Nursing, Kitami, Japan.

Introduction

POU1F1/PIT-1, a member of the POU family of transcription factors, is essential for pituitary growth and development.[1–3] POU1F1 also regulates cell-specific gene expression of somatotropes, lactotropes and thyrotropes, and is thus responsible for restricted expression of the corresponding pituitary hormones, GH, PRL and TSH. Previous studies have shown that the promoters of these genes contain a number of POU1F1-binding sites.[2] However, because POU1F1 is present in all three cell types, interactions with other transcription factors [e.g. oestrogen receptor (ER), thyroid hormone receptor (TR), Zn-15, Ets-1, GATA-2, Oct-1 and POU1F1 itself], as well as with transcriptional cofactors [e.g. cAMP-response element–binding protein–binding protein (CBP) and nuclear receptor corepressor (NcoR)], are vital to achieving their selective and targeted expressions.[2,4]

The predominant isoform of POU1F1, POU1F1-α/PIT-1α, is a 291-amino acid (aa) protein containing three important functional motifs: (i) an amino-terminal transactivation domain (TAD; spanning 8–80 aa of the human protein), (ii) a POU-specific domain (POU-S, 128–198 aa) that is unique to this class of transcription factors, and (iii) a carboxy-terminal POU homeodomain (POU-HD, 214–273 aa).[1,5,6] Previous studies suggested that TAD can be further divided into two subregions, R1 (8–45 aa) and R2 (46–80 aa), each encoded mainly by exons 1 and 2, respectively. Functional mapping demonstrated TAD-R1 to be responsible for basal transcriptional activity, whereas TAD-R2 consists of the strong activation region (50–70 aa) as well as the inhibitory/Ras-responsive region (70–80 aa) that is also implicated in interactions with other transcriptional corepressors and coactivators (e.g. ER and TR).[7,8]

Both POU-S and POU-HD contain helix-turn-helix DNA-recognition motifs, and they together constitute a bipartite DNA-binding structure essential for site-specific, high-affinity DNA binding of POU1F1 as well as for its dimer formation and specific protein–protein interactions.

In mammals, including humans, two minor POU1F1 isoforms, POU1F1-β/PIT-1β and PIT-1T, have been identified.[9–12] Both are generated by the alternative use of the splice acceptor site for exon 2, and thus, as compared to POU1F1-α, they only differ by additional aa residues (26 and 14 aa, for POU1F1-β and PIT-1T, respectively) inserted between the R1 and R2 subregions. Nevertheless, POU1F1-β and PIT-1T have been described as exhibiting different expression patterns and unique transcriptional properties. As opposed to POU1F1-α, POU1F1-β suppresses *GH*, *PRL* and *TSHβ* promoters in a pituitary-specific manner, blocking Ras-induced *PRL* promoter activity, whereas PIT-1T appears to be a thyrotrope-specific isoform required for optimal *TSHβ* promoter activation.

In murine models, a point mutation (p.W261C) or a genetic rearrangement (Pit-1^{dw}) in the *Pou1f1* gene results in dwarfism and anterior pituitary hypoplasia with Gh, Prl and Tsh deficiencies.[13,14] In humans, a number of *POU1F1* mutations have been described in a subset of patients with combined pituitary hormone deficiency (CPHD; MIM 613038).[3,4] In CPHD patients with *POU1F1* mutations, deficiencies of GH and PRL are generally complete and present early in life, whereas TSH deficiency can be more variable. The production of ACTH, LH and FSH is preserved. Brain magnetic resonance imaging (MRI) may show a normal or hypoplastic anterior pituitary. The majority of *POU1F1* mutations identified to date show recessive inheritance; however, at least six (p.P14L, p.P24L, p.Q167K, p.K216E and p.R271W) are reportedly inherited in a dominant manner with highly variable penetrance. Of these, p.R271W is the most frequent, having been identified in different ethnic groups. It has been suggested that the p.R271W form of POU1F1 may impair dimerization and act as a dominant-negative inhibitor of the wild-type POU1F1.[15]

In the present study, we describe the identification and characterization of a novel splice site mutation (Ex2 + 1G>T) of the *POU1F1* gene, which is found in a heterozygous state in Japanese identical twin brothers presenting an exceptionally mild CPHD phenotype. The mutation most likely leads to skipping of exon 2, and generation of a mutant protein, POU1F1 Δ48-72, which merely lacks most of the TAD-R2 subregion. *In vitro* functional study of the mutated protein showed only modest reductions in its transactivation activity in nonpituitary cells, while potentially acting in a dominant-negative manner on the endogenous activity of POU1F1 in pituitary cells.

Subjects and methods

Patients

This study was approved by the Ethics Committee for Human Genome/Gene Research at the University of Tokushima. Patients were recruited as part of the study of the Japan Growth Genome Consortium for genetic analysis of Japanese families with hereditary short stature.[16,17] After obtaining written informed consent, genomic DNA was extracted from peripheral blood leucocytes. DNA from 188 unrelated healthy Japanese subjects (94 women and 94 men) was used for mutation controls.

DNA analysis

The six *POU1F1*-coding exons and their flanking intronic regions, as well as the putative promoter, were analysed by sequencing. Primer sequences are shown in Table S1-1 and 2. PCR and sequencing reactions were performed as described previously.[16,17] The frequency of the Ex2 + 1G>T mutation in control subjects was determined using a mismatched-primer PCR-RFLP assay. PCR was carried out using primers hPOU1F1_F2NF (Table S1-1) and hPOU1F1_Int2_RFLP_R1: 5′-TCCCCAAATTCAATAACATG-TAAAAGACAACTTTggTTA-3′ (lower-case letters indicate the mismatched bases). Digestion of the wild-type allele with *Bst*EII (NEB, Beverly, MA, USA) yielded two fragments (268 and 40 bps), whereas the mutant allele was identified by the presence of undigested fragments (308 bp).

Cell cultures

HEK293T and COS-7 cells were maintained in DMEM (Invitrogen, Tokyo, Japan) supplemented with 10% foetal bovine serum (FBS) and antibiotics. Rat GH3 cells were grown in DMEM/F12 (Invitrogen) supplemented with 10% horse serum, 2·5% FBS and antibiotics.

Heterologous splicing assay

The *POU1F1* exon 2 and its flanking intronic sequence (675 bp) were amplified by PCR from the DNA of an affected individual and a control subject (Table S1-3), subcloned into the pSPL3 vector (Invitrogen), and designated as pSPL3-POU1F1-Ex2-WT or pSPL3-POU1F1-Ex2-MUT. Splicing assays were performed in HEK293T or COS-7 cells (1×10^6 cells/6-cm dish), which were transfected with 8 μg of plasmid DNA using FuGENE HD (Roche, Indianapolis, IN, USA). Forty-eight hours later, total RNA was isolated using an RNeasy Mini kit (Qiagen, Valencia, CA, USA) and reverse-transcribed using Superscript III (Invitrogen). Spliced products were detected by PCR with the primer combination SD6 and SA2 (vector-specific set), or exon 2-specific F1/F2 and SA2 (Table S1-4). Amplification of *β-actin* mRNA was used to assess reaction efficiency.

Expression and promoter–reporter constructs

A wild-type human POU1F1 expression vector, POU1F1-WT-pcDNA3, was provided by Dr Y. Okimura (Kobe Women's University). An in-frame deletion of exon 2 was incorporated into the POU1F1-WT-pcDNA3 using a KOD-Plus-Mutagenesis kit (Toyobo, Osaka, Japan) and designated as POU1F1-Δ48-72-pcDNA3. Full-length p300 and CBP expression vectors were gifts from Dr S. Ishii (RIKEN). Luciferase reporter constructs, rPRL0.6-Luc-pGL3 and rGH0.6-Luc-pGL3, containing either the rat *Prl* (−484 to +16664 relative to the transcription start site) or the rat *Gh* (−555

to +64) promoter sequence, were created by PCR amplification of the corresponding regions and subcloning into a pGL3-Basic plasmid (Promega, Madison, WI, USA). Oligonucleotide sequences used are shown in Table S1-5 and 6.

Immunoblotting

Western blotting of whole-cell lysates from GH3 or transfected HEK293T cells was carried out according to the standard procedure. Subcellular fractionation of transfected cells was performed using the NE-PER kit (Pierce, Rockford, IL, USA). The following primary antibodies were used: anti-PIT-1 (1:1000 dilution; SCB, Santa Cruz, CA, USA), anti-p62 (1:2000; BD Biosciences, San Jose, CA, USA), anti-PARP (1:1000; CST, Tokyo, Japan), anti-GAPDH (1:4000; Clontech-Takara, Kyoto, Japan) and anti-Actin (1:5000; Sigma, St. Louis, MO, USA) antibodies.

Indirect immunofluorescence

Immunofluorescence staining of transfected HEK293T cells was performed as described previously,[16] using anti-PIT-1 antibody (1:100) and Alexa Fluor 546-conjugated goat anti-rabbit IgG (1:200; Invitrogen) as the primary and secondary antibodies, respectively.

Luciferase reporter gene assay

HEK293T cells were seeded on collagen-coated 24-well plates (Iwaki, Nagoya, Japan) 1 day before transfection (5×10^4 cells/well), after which the reporters (pGL3 250 ng, pRL-TK 12·5 ng) and POU1F1-WT or Δ48-72 expression plasmid (250 ng) were introduced into cells at a 3:1 ratio of FuGENE HD (μl) to DNA (μg). Forty-eight hours after transfection, the cells were lysed and analysed for luciferase activity using a Dual-Luciferase Reporter Assay System (Promega). To improve efficiency in GH3 cells, which are refractory to transient transfection, these cells (1×10^5 cells/well) were transfected in suspension immediately after trypsinization at a 5:1 ratio of FuGENE HD to DNA, and the assay was performed 72 h later.

Electrophoretic mobility shift assay

Electrophoretic mobility shift assay (EMSAs) were performed using nuclear extracts from GH3 or transfected HEK293T cells, as described previously.[17] The unlabelled and biotin-labelled human hGHRHR-P2 probes (the sense sequence, 5′-ATCCTGGTGAATATTCAGCGGTCT-3′) and those derived from the rat *Prl* P3 promoter sequence[18] (rPRL-P3; Panomics, Redwood City, CA, USA) were utilized.

Statistical analysis

Data are presented as means ± SD. Statistical significance was analysed employing the two-tailed unpaired *t*-test for comparisons between control and experimental groups. $P < 0{\cdot}05$ was considered statistically significant.

Results

Case report

In September 1993, 5-year-old identical twin brothers (Family F: II.1 and II.2; Fig. 1a) were referred to the paediatric endocrinology clinic of the Asahikawa Medical University Hospital to determine the aetiology of their short stature. They were the first children of unrelated Japanese parents, born by caesarean section on the first day of the 38th week of gestation. Both parents were healthy, and

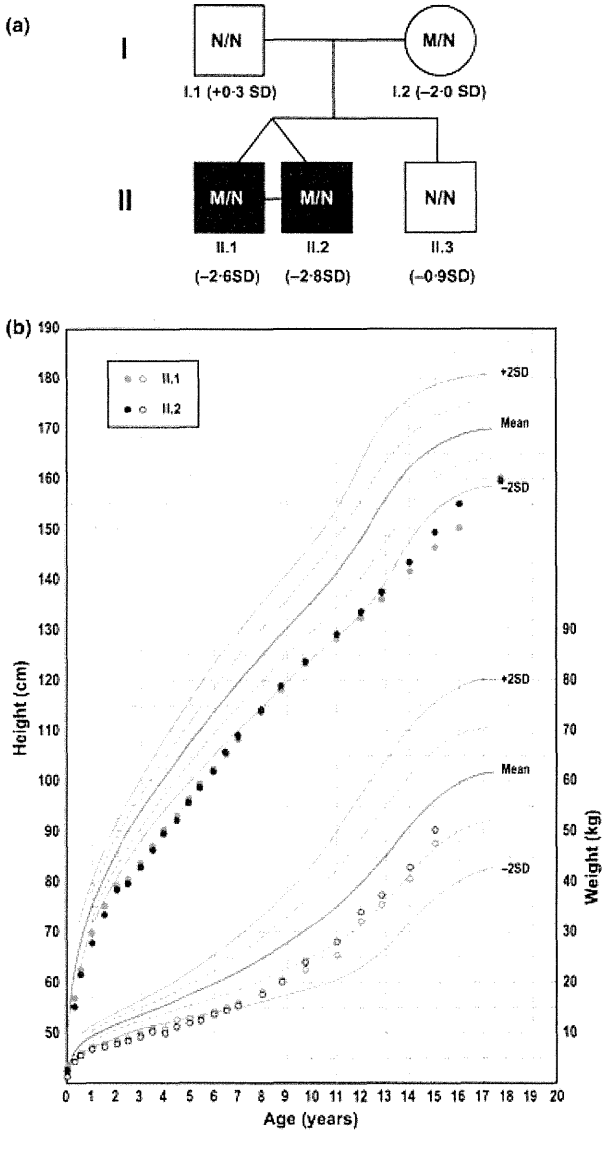

Fig. 1 Pedigree of Family F. (a) Pedigree of Family F with the *POU1F1* Ex2 + 1G>T mutation. Black filled symbols identify index cases. Males, squares; females, circles; M, mutated allele; N, normal allele. (b) Growth curves of patients II.1 and II.2. Heights and body weights are plotted on the Cross-Sectional Growth Chart 1990[30] for Japanese boys (0–18 years old). Closed and open circles (red, II.1; green, II.2) indicate the height and weight of the patients, respectively.

the father had a normal adult height (I.1: 37 years old, 172·1 cm/+0·3 SD), whereas the mother was rather small in stature (I.2: 38 years old, 148·0 cm/−2·0 SD). At birth, the patients were found to be small for gestational age (birth length and weight of II.1: 44·6 cm/−2·3 SD and 2364 g/−1·8 SD and II.2: 43·0 cm/−3·1 SD and 1942 g/−2·9 SD). They had episodes of transient neonatal hypoglycaemia and hyperbilirubinaemia. The mother had no medical history of hypothyroidism. After delivery, she had breastfed both infants without problems, but soon switched to formula feeding because she developed post-transfusion hepatitis. At the first hospital visit, the patient's heights were more than 2·5 SD below the average for boys of their age, and bone ages were delayed more than 2 years behind chronological age (Table 1). Results of hormonal evaluation indicated that they had partial GH deficiency, showing blunted GH peak responses (<6 ng/ml) to at least two different stimuli but more than 3 ng/ml to all stimuli on the GH provocative tests, together with decreased serum IGF-1 levels. Their serum IGFBP-3 levels were not measured. Basal and TRH-stimulated levels of PRL were low in both brothers. Basal free T4 and TSH levels were within normal range, and the peak TSH responses after TRH stimulation were normal or slightly blunted. Their serum LH and FSH levels were in the prepubertal range both before and after LHRH stimulation. Neither basal nor stimulated levels of ACTH and cortisol were measured. No brain MRI data were obtained for either patient. Based on the clinical and endocrinological findings, they were diagnosed as having partial CPHD, with mild GH and PRL deficiencies and borderline TSH deficiency. They had no or only mild symptoms. Eventually, it was decided that medical therapy, including GH and levothyroxine administration, was not necessary. The constructed growth chart showed similar growth curves for the brothers throughout the entire period of growth and indicated lack of a pubertal growth spurt (Fig. 1b). Their final heights were II.1: 160·4 cm/−1·8 SD and II.2: 159·8 cm/−1·9 SD. A younger brother's height was within normal range (II.3: 135·8 cm/−1·5 SD at age 11 years). In May 2011, the 56-year-old mother agreed to donate blood samples. Her laboratory tests yielded the following results: basal GH 0·07 ng/ml [reference range (RR) 0·28–1·64], IGF-1 89 ng/ml (−1·37 SD; RR 74–208), IGFBP −3 1·76 μg/ml (RR 1·99–3·19), PRL 1·38 ng/ml (RR 6·12–30·5), TSH 1·84 μIU/ml (RR 0·50–5·00), free T3 3·36 pg/ml (RR 2·30–4·30), free T4 1·08 ng/ml (RR 0·90–1·70), cortisol 9·0 μg/ml (RR 4·0–18·3) and ACTH 9·8 pg/ml (RR 7·2–63·3). Thus, her data were at least suggestive of mild GH and PRL deficiencies, similar to the clinical presentations of her affected sons, but a definitive diagnosis could not be established owing to lack of GH secretion data and brain MRI.

A novel Ex2 + 1G>T mutation in the POU1F1 gene affects splicing of exon 2

In both affected brothers of Family F, a heterozygous Ex2 + 1G>T (c.214 + 1G>T) mutation of *POU1F1* was identified (Fig. 2a). This nucleotide change disrupted a highly conserved GT dinucleotide sequence of the splice donor site at the exon 2–intron 2 boundary. The Ex2 + 1G>T mutation was also heterozygous in their mother (I.2; Fig. 2b), but was not found in the father or a younger brother, or in any of the 188 Japanese controls.

The effect of Ex2 + 1G>T on *in vitro* splicing efficiency was examined using minigene constructs, POU1F1-Ex2-WT and Ex2-MUT (Fig. 2c). When transfected into HEK293T cells, subsequent RT-PCR analysis using vector-derived primers SD6 and SA2 showed that POU1F1-Ex2-WT produced two splice products (Fig. 2d, top panel): a prominent 332-bp band reflecting exon 2 inclusion and a very faint 410-bp product resulting from alternative use of the exon 2 splice acceptor site (i.e. *POU1F1-β* isoform). On the other hand, POU1F1-Ex2-MUT generated only one product that did not contain exon 2. When using SA2 and *POU1F1*-specific primers (F1 and F2), a clear single band corresponding to the normally spliced products (F2 × SA2) as well as a faint band representing the *POU1F1-β* isoform (F1 × SA2) were observed for POU1F1-Ex2-WT, but these were not detected for Ex2-MUT (Fig. 2d, middle panels). Similar observations were also made after transfecting COS-7 cells (data not shown). Thus, our data suggested that Ex2 + 1G>T results in a large decrease in splicing efficiency

Table 1. Clinical and hormone data at initial presentation

									GH peak (ng/ml)	TSH (μIU/ml)	PRL (ng/ml)	LH (mIU/ml)	FSH (mIU/ml)
Subject	Sex	Age (years)	Height (cm)	Weight (kg)	BA (years)	Free T4 (ng/dl)	IGF-1 (ng/ml)	T (ng/dl)	Arg; Ins; L-dopa; GHRH	Baseline; under TRH	Baseline; under TRH	Baseline; under LHRH	Baseline; under LHRH
II.1	M	5·5	98·7 (−2·6 SD)	13·1 (−1·9 SD)	3·4	1·67	20	<5	5·04; 3·90; 6·64; 9·47	1·23; 12·5	0·95; 4·77	0·23; 4·02	1·40; 6·32
II.2	M	5·5	97·9 (−2·8 SD)	12·9 (−2·0 SD)	3·2	1·60	20	<5	8·34; 4·76; 4·67; 12·7	1·35; 14·4	0·94; 6·00	0·26; 3·87	1·94; 6·24
II.3	M	1·1	73·0 (−0·9 SD)	n/a	n/a	n/a	n/a	n/a	n/a	n/a	n/a	n/a	n/a

BA, bone age using the radius–ulna–short bones (RUS) method; T, testosterone; Arg, arginine; Ins, insulin; n/a, not available. Serum GH concentrations were measured using an IRMA kit (Daiichi Radioisotope Laboratories, Tokyo, Japan), and the original GH values (II.1, 8·07; 6·25; 10·6; 15·1; II.2, 13·3; 7·62; 7·48; 20·3) were corrected using the formula recommended by the Foundation for Growth Science in Japan to obtain the approximate values based on the International Standard of recombinant human GH. Reference values for age are as follows: free T4, 1·1–2·6; IGF-1, 29–173; testosterone, <10; GH peak, >6 (arginine, insulin, L-dopa and GHRH); TSH, 0·3–3·5 (baseline), 15–35 (under TRH); PRL, 1·7–15·4 (baseline), 29·4–35·8 (under TRH); LH, 0·2–1·2 (baseline); FSH 1·4–3·0 (baseline).

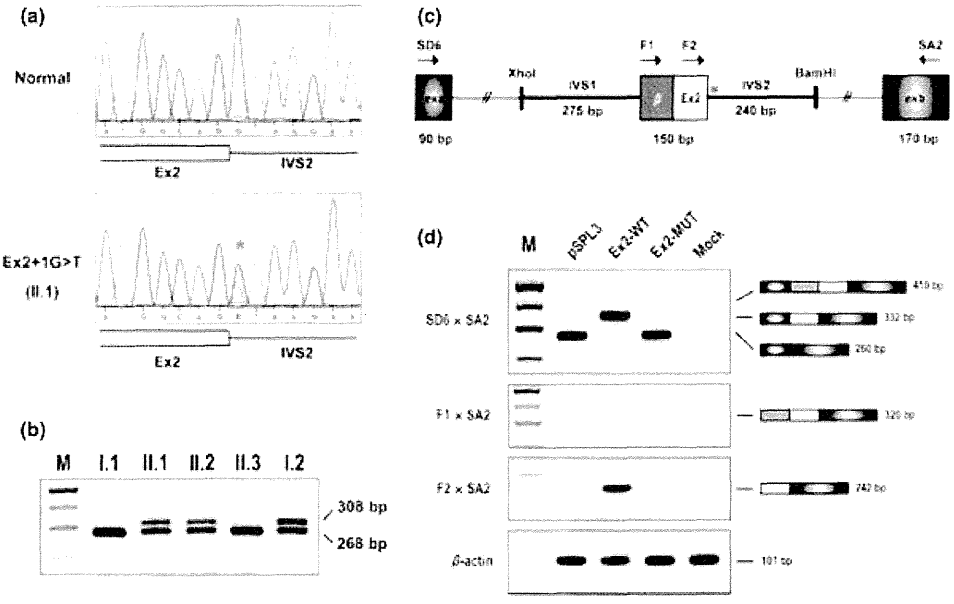

Fig. 2 A novel heterozygous Ex2 + 1 G>T splicing mutation in the *POU1F1* gene. (a) Sequence chromatograms display a portion of the exon 2–intron 2 boundary from a control individual (upper panel) and the index patient in Family F (II.1, lower panel). Patient F: II.1 has a heterozygous G>T transition (red asterisk) at position 1 of intron 2 (Ex2 + 1G>T), which abolishes the canonical donor splice site (GT dinucleotides). Ex, exon; IVS, intervening sequence. (b) In a mismatch PCR-RFLP assay, digestion of a 308-bp amplicon with BstEII yields 268- and 40-bp fragments (the 40-bp fragment is too short to be visible on the agarose gel). This mutation abolishes the BstEII site, and the 308-bp fragment remains intact (II.1, II.2 and I.2). Shown is a black/white inverted image of a gel stained with ethidium bromide. M, DNA size marker. (c) Representation of the pSPL3-POU1F1-Ex2-WT (wild-type) or Ex2-MUT (mutant) minigene constructs. A genomic fragment, containing *POU1F1* exon 2 (150 bp) and 275 bp of the 5′- and 240 bp of the 3′-intronic flanking sequence, was subcloned into the XhoI/BamHI site of pSPL3. Open box, exon 2 of *POU1F1*; grey box, an extended exon 2β specific for the POU1F1-β isoform; shaded boxes, pSPL3 vector exons, exa and exb; horizontal arrows, vector-derived primers SD6 and SA2, and exon 2-specific primers, F1 and F2. Note that primer F1 is specific to the *POU1F1-β* isoform, whereas F2 is common to both the α and the β isoform. Mutation site is indicated by an asterisk. (d) *In vitro* splicing assay. HEK293T cells were transiently transfected with POU1F1-Ex2 minigene constructs or empty pSPL3 vector (negative control). Subsequent RT-PCR analysis was performed with four different sets of primers. Top panel, amplicons obtained with the primer pair SD6/SA2. Note that the Ex2-WT construct yielded two bands of 332 and 410 bps that correspond to the inclusion of exons 2 and 2β respectively, while only a 260-bp band was generated by the Ex2-MUT or empty vectors. Middle panels, the primer pairs F1/SA2 or F2/SA2 produced the normally spliced products from the Ex2-WT construct, but no band is seen in the Ex2-MUT construct. Lower panel, RT-PCR products for β-actin (a RT-PCR quality control) are shown. Black/white inverted images are shown.

and in skipping of exon 2, rather than in the activation of a cryptic donor splice site.

POU1F1-Δ48-72 construct does not affect nuclear targeting and DNA binding in HEK293T cells

As our *in vitro* splicing assay results indicated that Ex2 + 1G>T causes an in-frame skipping of this exon, we generated a mutant expression construct with deletion of exon 2 (POU1F1-Δ48-72), and its functional properties were compared with those of the wild-type construct (POU1F1-WT). Immunoblotting of total cell lysates from POU1F1-WT-transfected HEK293T cells with a POU1F1-specific antibody revealed 33- and 31-kDa immunoreactive bands, arising from alternative translation initiation codon usage of *POU1F1* mRNA,[19] at levels similar to endogenous proteins in GH3 cells (Fig. S1). On the other hand, two smaller bands, 30 and 28 kDa, corresponding to forms with exon 2 deletion, were detected in cells transfected with POU1F1-Δ48-72.

We next examined whether Δ48-72 affects nuclear localization of POU1F1. Subcellular fractionation of POU1F1-WT or Δ48-72-expressing HEK293T cells followed by immunoblotting showed strong nuclear localization in each case (Fig. 3a). Consistently, immunocytochemical staining for POU1F1 showed virtually identical, intense nuclear staining for both WT and Δ48-72 forms (Fig. 3b).

We further performed EMSAs using two different EMSA probes containing previously characterized POU1F1-binding sites, one specific for the distal P2-binding element of the human *GHRHR* promoter (hGHRHR-P2)[17] and the other from the rat *Prl* proximal 3P region (rPRL-P3).[18] Nuclear extracts from POU1F1-WT-expressing cells formed a distinct DNA–protein complex in both cases (Fig. 3c), which was confirmed by supershift with anti-POU1F1 antibody. Similar EMSA results were obtained in nuclear extracts from the POU1F1-Δ48-72-expressing cells, suggesting DNA-binding activity to be unaffected by the mutation.

POU1F1-Δ48-72 exhibits reduced but not abolished transactivation capacity and an impaired synergic interaction with p300 in HEK293T cells

To characterize the effect of Δ48-72 on the function of POU1F1 in transactivation of target promoters, HEK293T cells were

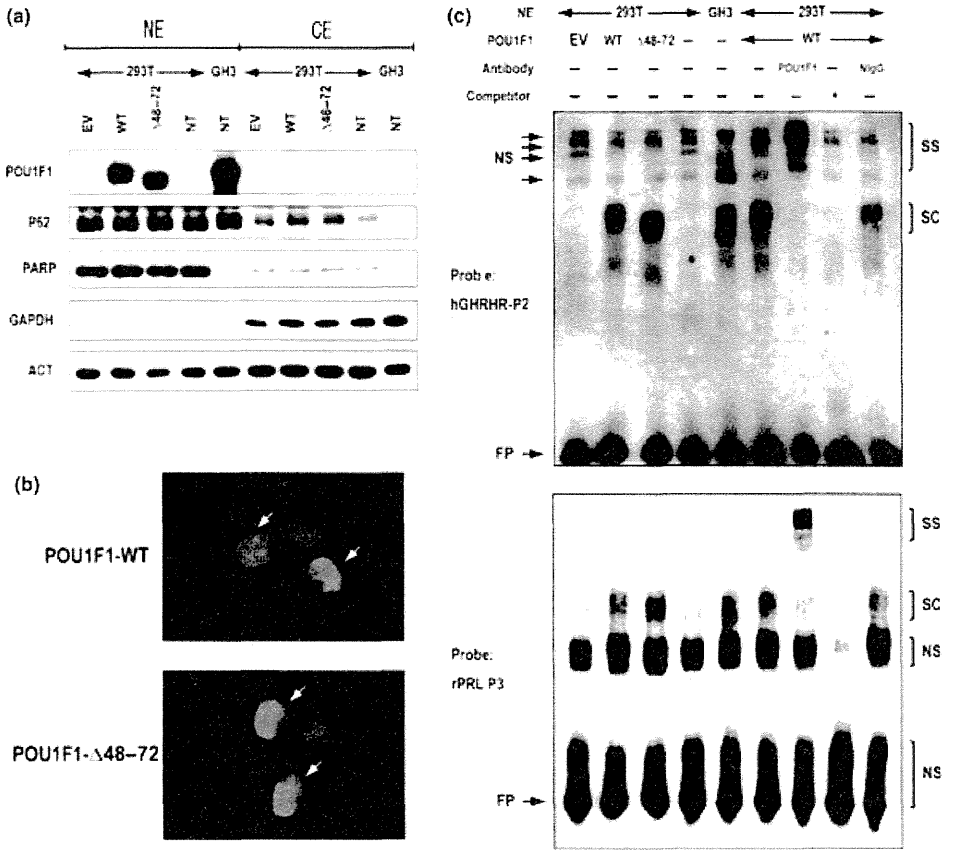

Fig. 3 The Δ48-72 mutant POU1F1 maintains normal nuclear targeting and DNA-binding ability. (a) HEK293T cells were transfected with wild-type (WT) or Δ48-72 mutant POU1F1, or empty vector (EV), and subjected to subcellular fractionation as described in Subjects and methods. As a control, the same procedures were carried out simultaneously with nontransfected (NT) 293T and GH3 cells. Equal amount of protein from either the nuclear (NE; 1 μg per lane) or the cytoplasmic (CE; 10 μg per lane) fractions were loaded on a 10–15% SDS-PAGE gel, transferred and reacted with anti-POU1F1 antibody. To assess the purity of the NE and CE fractions, immunoblot analysis was also conducted with antibodies against nuclear (p62 and PARP) and cytoplasmic (GAPDH) marker proteins. Actin (present in both NE and CE fractions) was probed as a loading control. (b) Indirect immunofluorescent localization of POU1F1 in HEK293T cells transiently transfected with POU1F1-WT (upper) or Δ48-72 (lower) expression constructs. Merged images of anti-POU1F1 (red) and DAPI (blue) are shown. White arrows indicate a nucleus positive for POU1F1, which appears pink as the red stain is overlaid with blue. (c) Electrophoretic mobility shift assays (EMSAs). Nuclear extracts (NE) from transfected HEK293T and GH3 (positive control) cells were prepared and subjected to EMSA with POU1F1-specific oligonucleotide probes (hGHRHR-P2 and rPRL-P3). Competition experiments were performed with unlabelled competitor probes at a 100-fold molar excess. For supershift experiments, antibodies specific for POU1F1 or normal IgG (NIgG; as a negative control) were used. SC indicates POU1F1-specific complex; SS, supershifted complex; NS, nonspecific bands and complex; FP, free probe.

cotransfected with various amounts of either POU1F1-WT or Δ48-72 expression constructs with luciferase reporter genes containing rat *Prl* or *Gh* proximal promoter sequences (rPRL0.6-Luc or rGH0.6-Luc). As shown in Fig. 4a, POU1F1-Δ48-72 showed significantly decreased, but not absent, transcriptional activity (61–81% to the WT activities). When cotransfected with WT, equivalent amounts of Δ48-72 did not inhibit instead additively activated rPRL0.6-Luc and rGH0.6-Luc activities (Fig. 4b), suggesting that Δ48-72 does not exhibit a dominant-negative effect in HEK293T cells.

CBP and p300 were previously described to act as coactivators of a large number of transcription factors, including POU1F1.[20] Consistently, cotransfection of the POU1F1-WT with either the CBP or p300 expression constructs resulted in a synergistic enhancement of transactivation of the rat *Prl* and *Gh* promoters (Fig. 4c). When POU1F1-Δ48-72 was cotransfected with CBP, a similar synergy was observed, whereas no such effects were seen with p300, suggesting the Δ48-72 mutant to be specifically defective in its ability to synergize with p300.

POU1F1-Δ48-72 displays a dominant-negative activity against endogenous POU1F1 and suppresses the rat Gh promoter activity in GH3 cells

Because previous studies suggested the possible cell type specificity of dominant-negative effects of some POU1F1 mutations, we sought to examine the effect of the Δ48-72 mutation against endogenous POU1F1 protein. For this purpose, we conducted reporter assays using GH3 somatolactotrope cells, which express *Pou1f1* as well as *Prl* and *Gh* genes. As shown in Fig. 5, the baseline reporter

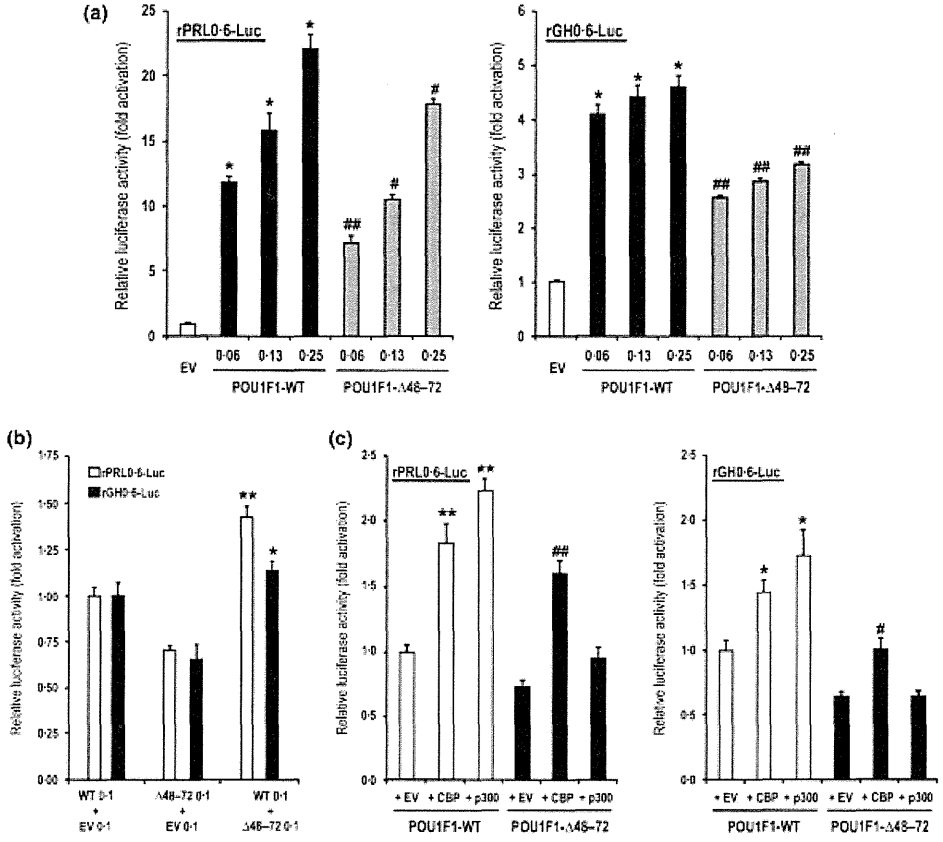

Fig. 4 Reduced transactivation ability and impaired synergy with p300 of the Δ48-72 POU1F1 form. A. HEK293T cells seeded in a 24-well plate were cotransfected with a reporter construct (rPRL0.6-Luc, left; rGH0.6-Luc, right panel), a renilla luciferase construct (pRL-TK, for normalization) and increasing amounts (0·06–0·25 μg DNA per well) of plasmid encoding wild-type (WT) or Δ48-72 mutant human POU1F1. Total amounts of transfected DNA were kept constant by adding empty vector pcDNA3 (EV) as appropriate. The cells were lysed 48 h after transfection, and luciferase activity was measured. Data were normalized and expressed as fold activation relative to the value of the 'EV only' control, which was set to 1. White bar, EV; black bars, POU1F1-WT; dark grey bars, POU1F1-Δ48-72. Each bar represents the mean ± SD of four determinations in one representative series of experiments out of three performed. The statistical significance of differences was determined using the two-tailed unpaired *t*-test. $^{*}P < 0{\cdot}0001$ *vs* EV, $^{\#}P < 0{\cdot}001$ and $^{\#\#}P < 0{\cdot}0001$ *vs* POU1F1-WT. (b) To assess whether the Δ48-72 mutant can inhibit the ability of the WT protein to transactivate the *GH* and *PRL* promoters, equal amounts (0·1 μg each per well of a 24-well plate) of POU1F1-WT and Δ48-72 plasmid DNAs were transfected into HEK293T cells along with either rPRL0.6-Luc or rGH0.6-Luc reporter plasmid, and luciferase assays were carried out. Cells transfected with POU1F1-WT or Δ48-72 alone, keeping the amount of DNA constant by addition of empty vector (EV), were compared. Data were normalized and expressed as fold activation relative to the values of the 'WT+EV' control, which were set to 1. White bar, rPRL0.6-Luc; black bars, rGH0.6-Luc. One representative experiment out of four is shown. $^{*}P < 0{\cdot}05$ and $^{**}P < 0{\cdot}0001$ *vs* WT+EV. (c) To evaluate the effects of the Δ48-72 mutation on the synergistic interactions between POU1F1 and either cAMP-response element binding protein–binding protein (CBP) or p300, as coactivators, on *GH* and *PRL* promoters, POU1F1-WT and Δ48-72 were transfected with either CBP or p300 expression constructs as indicated, along with either rPRL0.6-Luc or rGH0.6-Luc. Luciferase assays were then performed. Relative luciferase activity is indicated as the mean ± SD fold activation relative to the value of the 'POU1F1-WT+EV' transfection (set to 1). A representative result from three independent experiments is shown, each performed in quadruplicate and each yielding similar results. $^{*}P < 0{\cdot}001$ and $^{**}P < 0{\cdot}0001$ *vs* EV, $^{\#}P < 0{\cdot}001$ and $^{\#\#}P < 0{\cdot}0001$ *vs* EV.

gene activities (cotransfected with empty vector) of the rPRL0.6-Luc and rGH0.6-Luc constructs were significantly elevated, reflecting endogenous gene expressions. Consistent with previous observations showing that cotransfection with wild-type POU1F1 elicited only marginal enhancements of target promoter activities in pituitary cells,[11,21] the introduction of POU1F1-WT into GH3 cells showed only small but significant increases in reporter gene activities, with maximum inductions of 1·22- and 1·17-fold for *Prl* and *Gh* promoters, respectively. Unlike with POU1F1-WT, transfection of POU1F1-Δ48-72 significantly suppressed rGH0.6-Luc activity in a dose-dependent manner (53·9% inhibition at the maximum dose), while suppressing rPRL0.6-Luc activity only at the highest dose (84·5% inhibition).

Discussion

The classification and distribution pattern of the disease-associated *POU1F1* mutations showed that the majority (approximately 60%) are missense mutations within the POU-S and POU-HD domains (Fig. S2, Table S2), encoded by exons 4 and 6, respectively. Meanwhile, only a few mutations specifically affecting the TAD region (e.g. p.P14L and p.P24L) have been described to date, and the same

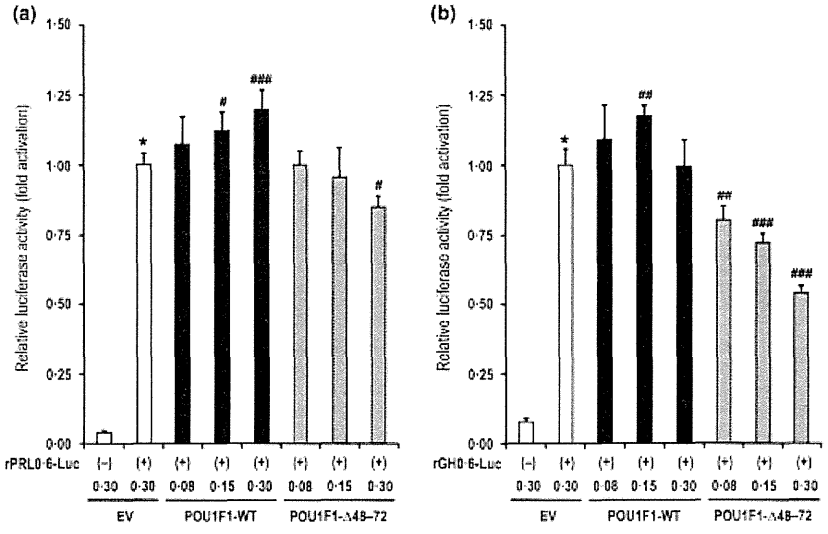

Fig. 5 The Δ48-72 mutant POU1F1 inhibits the activities of the *PRL* and *GH* promoters in GH3 cells. GH3 cells seeded in a 24-well plate were transfected with the rPRL0.6-Luc or rGH0.6-Luc constructs and indicated amounts (μg) of expression vectors encoding POU1F1-WT and POU1F1-Δ48-72, or EV, using an optimized cell-specific protocol (see Subjects and methods). The pRL-TK vector was also used as an internal control, pGL3-Basic as a negative control. Cells were harvested 72 h after transfections, and luciferase activities were measured. Relative luciferase activity is indicated as the mean ± SD fold activation relative to the value of each reporter without POU1F1-WT and POU1F1-Δ48-72 transfections (set to 1). A representative result from three independent experiments is shown, each performed in quadruplicate and each yielding similar results. The statistical significance of differences was determined using the two-tailed unpaired *t*-test. $^{*}P < 0{\cdot}0001$ *vs* empty pGL3-Basic (–), $^{\#}P < 0{\cdot}01$, $^{\#\#}P < 0{\cdot}001$ and $^{\#\#\#}P < 0{\cdot}0001$ *vs* EV.

is true for those involving specific splice sites. To our knowledge, Ex2 + 1G>T is the first demonstration of a mutation specifically involving exon 2, thus affecting TAD, and one of the few examples of aberrant splicing mutations of *POU1F1*.

The *in vitro* splicing assay suggested that Ex2 + 1G>T causes an in-frame skipping of exon 2 in the mRNA, thus generating an internally deleted protein, lacking nearly four-fifths (aa 48–72) of the TAD-R2 subdomain. Functional analysis of POU1F1-Δ48-72 showed reduced but not abolished ability to transactivate the rat *Prl* and *Gh* promoters, with an impaired synergistic interaction with p300, in nonpituitary HEK293T cells. In contrast, dominant-negative activity was exhibited against endogenous POU1F1 in GH3 somatolactotrope cells. These data are generally consistent with previous studies, which suggested the TAD-R2 subregion, as a whole, to play only a contributory role in basal transcriptional activity, although it is likely to be crucial for transcriptional synergy with other transcriptional cofactors (e.g. ER and TR) and, in a similar way, for Ras responsiveness.[7,22–24] A previous report also revealed a motif containing three tyrosine residues separated by six aa residues (Y6Y6Y) encoded by exon 2 to be critical for these effects.[7] In addition, the potential dominant-negative effects of several *POU1F1* mutations have been extensively investigated, and it was emphasized that such effects are largely dependent on experimental conditions and likely to be detectable only in a cell type- or promoter-specific manner.[25,26] The p.R271W mutation was initially found to dominantly inhibit the activation of the *GH* and *PRL* genes by wild-type POU1F1,[27] although this was later disputed.[28] In a more recent study, however, the dominant-negative effects of p.R271W were shown to be detectable only in cells possessing an endogenous POU1F1.[26] In the case of p.K216E, the mutation was found not only to be a superactive stimulator of *GH* and *PRL* promoter activities in nonpituitary CV-1 cells but also to inhibit retinoic acid-induced upregulation of *Pou1f1* expression in GH3 cells.[29]

It should be noted that, in the majority of previously described CPHD patients with *POU1F1* mutations, GH and PRL deficiencies were usually complete, leading to early and progressive growth failure and severe short stature, while the time of onset and the degree of TSH deficiency could be variable. In addition, recessive *POU1F1* mutations reportedly show no obvious phenotype when heterozygous. In this context, our patients had relatively mild short stature and represented a state of partial, rather than an absolute, deficiency of GH. We assume that a similar situation likely occurred in their undiagnosed mother who also presented with mild short stature and harboured the same mutation; however, detailed evaluations including the GH provocative tests and brain MRI are obviously needed before a definitive diagnosis can be established. While a single Ex2 + 1G>T mutation was detected in only one allele of these patients, this mutation falls outside the *POU1F1* mutational hotspot domains, POU-S and POU-HD, and has the potential to act as a dominant-negative inhibitor of endogenous POU1F1. We thus speculate that the rather unusually mild CPHD phenotype of our patients may be attributable to these unique features in mutational location and type of Ex2 + 1G>T. It is also noteworthy that Ex2 + 1G>T is expected to simultaneously disrupt the POU1F1-β and PIT-1T isoforms, containing different 5′-extended variants of exon 2, which are believed to play distinctive and important roles in the regulation of POU1F1-dependent promoters.[11,12] The Ex2 + 1G>T mutation may contribute to the unique clinical phenotypes of our patients in this

regard; however, further experimental evidence is needed to support this hypothesis.

In summary, we have described herein the first identified splice site mutation (Ex2 + 1G>T) at the exon 2–intron 2 splice junction of the *POU1F1* gene, which occurred in heterozygous form in identical twin brothers presenting mild CPHD. The addition of this mutation to the growing list of pathological *POU1F1* mutations may provide meaningful insights into clinical heterogeneity in the expression of individual mutations and a deeper understanding of the structure–function relationships of the POU1F1 protein.

Acknowledgements

We acknowledge the resources provided by the Japan Growth Genome Consortium, and the participating patients and their family members. We would like to thank Professor Yasuhiko Okimura (Kobe Women's University, Kobe, Japan) and Professor Shunsuke Ishii (Tsukuba Life Science Center, RIKEN, Japan) for providing us their expression plasmids. This work was supported by a research grant from Novo Nordisk. This paper is dedicated to Professor Kenji Fujieda who passed away on 19 March 2010 during the completion of this work. Japan Growth Genome Consortium: Department of Paediatrics, Asahikawa Medical College; Department of Endocrinology and Metabolism, National Research Institute for Child Health and Development; Saitama Children's Medical Center; Department of Paediatrics, Hokkaido University Graduate School of Medicine; Department of Paediatrics, Tendo City Hospital; Department of Paediatrics, University of Yamanashi School of Medicine; Department of Paediatrics, Fukui Medical University; Department of Paediatrics, Japanese Red Cross Society Wakayama Medical Center; Department of Paediatrics, Odawara Municipal Hospital; Department of Paediatrics, Graduate School of Medicine, Kyoto University; Department of Paediatrics, Niigata Prefectural Shibata Hospital; Department of Paediatrics, Keio University School of Medicine; Department of Paediatrics, Nagasaki University School of Medicine; Department of Paediatrics, Tottori University Hospital; Department of Paediatrics, Fujieda Municipal General Hospital; Department of Paediatrics, Hiroshima University Hospital; Department of Paediatrics, Kawasaki Municipal Hospital; Department of Paediatrics, Akita Kumiai General Hospital; Igarashi Children's Clinic; Department of Paediatrics, Tokyo Denryoku Hospital; Department of Paediatrics, Hamamatsu University School of Medicine; Department of Paediatrics, Shinsyu University Hospital; Department of Paediatrics, Ehime University Graduate School of Medicine; Institute for Genome Research, The University of Tokushima.

Disclosure

The authors have no conflicts of interest to declare.

References

1 Andersen, B. & Rosenfeld, M.G. (1994) Pit-1 determines cell types during development of the anterior pituitary gland. A model for transcriptional regulation of cell phenotypes in mammalian organogenesis. *The Journal of Biological Chemistry*, **269**, 29335–29338.

2 Andersen, B. & Rosenfeld, M.G. (2001) POU domain factors in the neuroendocrine system: lessons from developmental biology provide insights into human disease. *Endocrine Reviews*, **22**, 2–35.

3 Kelberman, D., Rizzoti, K., Lovell-Badge, R. *et al.* (2009) Genetic regulation of pituitary gland development in human and mouse. *Endocrine Reviews*, **30**, 790–829.

4 Cohen, L.E. & Radovick, S. (2002) Molecular basis of combined pituitary hormone deficiencies. *Endocrine Reviews*, **23**, 431–442.

5 Theill, L.E., Castrillo, J.L., Wu, D. *et al.* (1989) Dissection of functional domains of the pituitary-specific transcription factor GHF-1. *Nature*, **342**, 945–948.

6 Ingraham, H.A., Flynn, S.E., Voss, J.W. *et al.* (1990) The POU-specific domain of Pit-1 is essential for sequence-specific, high affinity DNA binding and DNA-dependent Pit-1-Pit-1 interactions. *Cell*, **61**, 1021–1033.

7 Holloway, J.M., Szeto, D.P., Scully, K.M. *et al.* (1995) Pit-1 binding to specific DNA sites as a monomer or dimer determines gene-specific use of a tyrosine-dependent synergy domain. *Genes & Development*, **9**, 1992–2006.

8 Duval, D.L., Jonsen, M.D., Diamond, S.E. *et al.* (2007) Differential utilization of transcription activation subdomains by distinct coactivators regulates Pit-1 basal and Ras responsiveness. *Molecular Endocrinology*, **21**, 172–185.

9 Theill, L.E., Hattori, K., Lazzaro, D. *et al.* (1992) Differential splicing of the GHF1 primary transcript gives rise to two functionally distinct homeodomain proteins. *The EMBO Journal*, **11**, 2261–2269.

10 Konzak, K.E. & Moore, D.D. (1992) Functional isoforms of Pit-1 generated by alternative messenger RNA splicing. *Molecular Endocrinology*, **6**, 241–247.

11 Jonsen, M.D., Duval, D.L. & Gutierrez-Hartmann, A. (2009) The 26-amino acid beta-motif of the Pit-1beta transcription factor is a dominant and independent repressor domain. *Molecular Endocrinology*, **23**, 1371–1384.

12 Haugen, B.R., Gordon, D.F., Nelson, A.R. *et al.* (1994) The combination of Pit-1 and Pit-1T have a synergistic stimulatory effect on the thyrotropin beta-subunit promoter but not the growth hormone or prolactin promoters. *Molecular Endocrinology*, **8**, 1574–1582.

13 Li, S., Crenshaw, E.B., Rawson, E.J. *et al.* (1990) Dwarf locus mutants lacking three pituitary cell types result from mutations in the POU-domain gene pit-1. *Nature*, **347**, 528–533.

14 Camper, S.A., Saunders, T.L., Katz, R.W. *et al.* (1990) The Pit-1 transcription factor gene is a candidate for the murine Snell dwarf mutation. *Genomics*, **8**, 586–590.

15 Jacobson, E.M., Li, P., Leon-del-Rio, A. *et al.* (1997) Structure of Pit-1 POU domain bound to DNA as a dimer: unexpected arrangement and flexibility. *Genes & Development*, **11**, 198–212.

16 Inoue, H., Kangawa, N., Kinouchi, A. *et al.* (2011) Identification and functional analysis of novel human growth hormone secretagogue receptor (GHSR) gene mutations in Japanese subjects with short stature. *The Journal of Clinical Endocrinology and Metabolism*, **96**, E373–E378.

17 Inoue, H., Kangawa, N., Kinouchi, A. *et al.* (2011) Identification and functional analysis of novel human growth hormone-releasing hormone receptor (GHRHR) gene mutations in Japanese subjects with short stature. *Clinical Endocrinology*, **74**, 223–233.

18 Yan, G.Z., Pan, W.T. & Bancroft, C. (1991) Thyrotropin-releasing hormone action on the prolactin promoter is mediated by the POU protein pit-1. *Molecular Endocrinology*, **5**, 535–541.

19 Voss, J.W., Yao, T.P. & Rosenfeld, M.G. (1991) Alternative translation initiation site usage results in two structurally distinct forms of Pit-1. *The Journal of Biological Chemistry*, **266**, 12832–12835.

20 Cohen, R.N., Brue, T., Naik, K. *et al.* (2006) The role of CBP/p300 interactions and Pit-1 dimerization in the pathophysiological mechanism of combined pituitary hormone deficiency. *The Journal of Clinical Endocrinology and Metabolism*, **91**, 239–247.

21 Ferry, A.L., Locasto, D.M., Meszaros, L.B. *et al.* (2005) Pit-1beta reduces transcription and CREB-binding protein recruitment in a DNA context-dependent manner. *Journal of Endocrinology*, **185**, 173–185.

22 Chang, W., Zhou, W., Theill, L.E. *et al.* (1996) An activation function in Pit-1 required selectively for synergistic transcription. *The Journal of Biological Chemistry*, **271**, 17733–17738.

23 Diamond, S.E., Chiono, M. & Gutierrez-Hartmann, A. (1999) Reconstitution of the protein kinase A response of the rat prolactin promoter: differential effects of distinct Pit-1 isoforms and functional interaction with Oct-1. *Molecular Endocrinology*, **13**, 228–238.

24 Duval, D.L., Jean, A. & Gutierrez-Hartmann, A. (2003) Ras signaling and transcriptional synergy at a flexible Ets-1/Pit-1 composite DNA element is defined by the assembly of selective activation domains. *The Journal of Biological Chemistry*, **278**, 39684–39696.

25 Turton, J.P., Reynaud, R., Mehta, A. *et al.* (2005) Novel mutations within the POU1F1 gene associated with variable combined pituitary hormone deficiency. *The Journal of Clinical Endocrinology and Metabolism*, **90**, 4762–4770.

26 Pellegrini, I., Roche, C., Quentien, M. *et al.* (2006) Involvement of the pituitary-specific transcription factor pit-1 in somatolactotrope cell growth and death: an approach using dominant-negative pit-1 mutants. *Molecular Endocrinology*, **20**, 3212–3227.

27 Radovick, S., Nations, M., Du, Y. *et al.* (1992) A mutation in the POU-homeodomain of Pit-1 responsible for combined pituitary hormone deficiency. *Science*, **257**, 1115–1118.

28 Kishimoto, M., Okimura, Y., Fumoto, M. *et al.* (2003) The R271W mutant form of Pit-1 does not act as a dominant inhibitor of Pit-1 action to activate the promoters of GH and prolactin genes. *European Journal of Endocrinology*, **148**, 619–625.

29 Cohen, L.E., Zanger, K., Brue, T. *et al.* (1999) Defective retinoic acid regulation of the Pit-1 gene enhancer: a novel mechanism of combined pituitary hormone deficiency. *Molecular Endocrinology*, **13**, 476–484.

30 Suwa, S. & Tachibana, K. (1993) Standard growth charts for height and weight of Japanese children from birth to 17 years based on a cross-sectional survey of national data. *Clinical Pediatric Endocrinology*, **2**, 87–97.

Supporting Information

Additional Supporting Information may be found in the online version of this article:

Fig. S1. Western blot analysis.

Fig. S2. Protein domains, genomic organization and pathogenic mutations of POU1F1.

Table S1. Sequence of oligonucleotides used in this study.

Table S2. List of CPHD-associated *POU1F1* mutations reported in the literature.

Please note: Wiley-Blackwell are not responsible for the content or functionality of any supporting materials supplied by the authors. Any queries (other than missing material) should be directed to the corresponding author for the article.

European Journal of Human Genetics (2012) 20, 928–932

www.nature.com/ejhg

EJHG Open

ARTICLE

Relative frequency of underlying genetic causes for the development of UPD(14)pat-like phenotype

Masayo Kagami[1], Fumiko Kato[1], Keiko Matsubara[1], Tomoko Sato[1], Gen Nishimura[2] and Tsutomu Ogata[*,1,3]

Paternal uniparental disomy 14 (UPD(14)pat) results in a unique constellation of clinical features, and a similar phenotypic constellation is also caused by microdeletions involving the *DLK1-MEG3* intergenic differentially methylated region (IG-DMR) and/or the *MEG3*-DMR and by epimutations (hypermethylations) affecting the DMRs. However, relative frequency of such underlying genetic causes remains to be clarified, as well as that of underlying mechanisms of UPD(14)pat, that is, trisomy rescue (TR), gamete complementation (GC), monosomy rescue (MR), and post-fertilization mitotic error (PE). To examine this matter, we sequentially performed methylation analysis, microsatellite analysis, fluorescence *in situ* hybridization, and array-based comparative genomic hybridization in 26 patients with UPD(14)pat-like phenotype. Consequently, we identified UPD(14)pat in 17 patients (65.4%), microdeletions of different patterns in 5 patients (19.2%), and epimutations in 4 patients (15.4%). Furthermore, UPD(14)pat was found to be generated through TR or GC in 5 patients (29.4%), MR or PE in 11 patients (64.7%), and PE in 1 patient (5.9%). Advanced maternal age at childbirth (≥35 years) was predominantly observed in the MR/PE subtype. The results imply that the relative frequency of underlying genetic causes for the development of UPD(14)pat-like phenotype is different from that of other imprinting disorders, and that advanced maternal age at childbirth as a predisposing factor for the generation of nullisomic oocytes through non-disjunction at meiosis 1 may be involved in the development of MR-mediated UPD(14)pat.
European Journal of Human Genetics (2012) **20**, 928–932; doi:10.1038/ejhg.2012.26; published online 22 February 2012

Keywords: genetic cause; maternal age effect; monosomy rescue; UPD(14)pat subtype

INTRODUCTION

Human chromosome 14q32.2 carries a ~1.2 Mb imprinted region with the germline-derived primary *DLK1-MEG3* intergenic differentially methylated region (IG-DMR) and the post-fertilization-derived secondary *MEG3*-DMR, together with multiple imprinted genes.[1,2] Both DMRs are methylated after paternal transmission and unmethylated after maternal transmission in the body, whereas in the placenta the IG-DMR alone remains as a DMR and the *MEG3*-DMR is rather hypomethylated irrespective of the parental origin.[2,3] Furthermore, it has been shown that the unmethylated IG-DMR and *MEG3*-DMR of maternal origin function as the imprinting centers in the placenta and the body, respectively, and that the IG-DMR acts as an upstream regulator for the methylation pattern of the *MEG3*-DMR in the body but not in the placenta.[3]

As a result of the presence of the imprinted region, paternal uniparental disomy 14 (UPD(14)pat) (OMIM #608149) causes a unique constellation of body and placental phenotypes such as characteristic face, bell-shaped small thorax, abdominal wall defect, polyhydramnios, and placentomegaly.[2,4,5] Furthermore, consistent with the essential role of the DMRs in the imprinting regulation, microdeletions and epimutations affecting the IG-DMR or both DMRs of maternal origin result in UPD(14)pat-like phenotype in both the body and the placenta, whereas a microdeletion involving the maternally inherited *MEG3*-DMR alone leads to UPD(14)pat-like phenotype in the body, but not in the placenta.[2,3]

Of the three underlying genetic causes for UPD(14)pat-like phenotype (UPD(14)pat, microdeletions, and epimutations), UPD(14)pat is primarily generated by four mechanisms, that is, trisomy rescue (TR), gamete complementation (GC), monosomy rescue (MR), and post-fertilization mitotic error (PE).[6] TR refers to a condition in which chromosome 14 of maternal origin is lost from a zygote with trisomy 14 formed by fertilization between a disomic sperm and a normal oocyte. GC results from fertilization of a disomic sperm with a nullisomic oocyte. MR refers to a condition in which chromosome 14 of paternal origin is replicated in a zygote with monosomy 14 formed by fertilization between a normal sperm and a nullisomic oocyte. PE is an event after formation of a normal zygote. In this regard, a nullisomic oocyte specific to GC and MR is produced by non-disjunction at meiosis 1 (M1) or meiosis 2 (M2), and non-disjunction at M1 is known to increase with maternal age, probably because of a long-term (10–50 years) meiotic arrest at prophase 1.[7]

However, relative frequency of the genetic causes for UPD(14)pat-like phenotype remains to be determined, as well as that of underlying mechanisms for the generation of UPD(14)pat. Here, we report our data on this matter, and discuss the difference in the relative frequency

[1]Department of Molecular Endocrinology, National Research Institute for Child Health and Development, Tokyo, Japan; [2]Department of Radiology, Tokyo Metropolitan Children's Medical Center, Fuchu, Japan; [3]Department of Pediatrics, Hamamatsu University School of Medicine, Hamamatsu, Japan
*Correspondence: Professor T Ogata, Department of Pediatrics, Hamamatsu University School of Medicine, Hamamatsu 431-3192, Japan. Tel: +81 53 435 2310; Fax: +81 53 435 2312; E-mail: tomogata@hama-med.ac.jp
Received 23 May 2011; revised 10 November 2011; accepted 26 December 2011; published online 22 February 2012

among imprinted disorders and the possible maternal age effect on the relative frequency.

PATIENTS AND METHODS

Patients

This study comprised 26 patients with UPD(14)pat-like phenotype (9 male patients and 17 female patients) (Table 1). Of the 26 patients, 18 patients have been reported previously; they consisted of nine sporadic patients with full UPD(14)pat,[4,5] one sporadic patient with segmental UPD(14)pat,[4] the proband of sibling cases and four sporadic patients with different patterns of microdeletions involving the unmethylated DMRs of maternal origin,[2,3] and three patients with epimutations (hypermethylations) of the two normally unmethylated DMRs of maternal origin.[2] The remaining eight patients were new sporadic cases.

Phenotypic findings of the 26 patients are summarized in Supplementary Table 1; detailed clinical features of patients 6 and 16–25 are as described previously,[2–4] and those of the eight new patients 3, 5, 10–14, and 26 are shown in Supplementary Table 2, together with those of patients 1, 2, 4, 7–9, and 15 in whom detailed phenotypes were not described in the previous report.[5] All the 26 patients were identified shortly after birth because of the unique bell-shaped thorax with coat-hanger appearance of the ribs on roentgenograms obtained because of asphyxia. Subsequent clinical analysis revealed that 25 of the 26 patients exhibited both body and placental UPD(14)pat-like phenotype, whereas the remaining one previously reported patient (patient 22) manifested body, but not placental, UPD(14)pat-like phenotype.[3] The karyotype was found to be normal in 25 patients, although cytogenetic analysis was not performed in one previously reported patient who died of respiratory failure at 2 h of age (patient 6).[4] One patient (patient 15) was conceived by *in vitro* fertilization-embryo transfer.[5] This study was approved by the Institute Review Board Committee at the National Center for Child Health and Development, and performed after obtaining written informed consent.

Analysis of underlying genetic causes in patients with UPD(14)pat-like phenotype

We sequentially performed methylation analysis, microsatellite analysis, and fluorescence *in situ* hybridization (FISH), using leukocyte genomic DNA samples and lymphocyte metaphase spreads of all the 26 patients with UPD(14)pat-like phenotype. The detailed methods were as reported previously.[2,3] In brief, methylation analysis was performed for the IG-DMR (CG4 and CG6) and the *MEG3*-DMR (CG7 and the CTCF-biding sites C and D) by combined bisulfite restriction analysis and bisulfite sequencing. Microsatellite analysis was performed for multiple loci on chromosome 14, by determining the sizes of PCR products obtained with fluorescently labeled forward primers and unlabeled reverse primers. FISH analysis was carried out for the IG-DMR and the *MEG3*-DMR using 5104-bp and 5182-bp long PCR products, respectively, together with the RP11-566I2 probe for 14q12 utilized as an internal control.

In this study, furthermore, oligonucleotide array-based comparative genomic hybridization (CGH) was also performed for the imprinted region of non-UPD(14)pat patients, using a custom-build oligo-microarray containing 12 600 probes for 14q32.2–q32.3 encompassing the imprinted region and ~10 000 reference probes for other chromosomal region (4×180K format, Design ID 032112) (Agilent Technologies, Palo Alto, CA, USA). The procedure was as described in the manufacturer's instructions.

Analysis of subtypes in patients with UPD(14)pat

UPD(14)pat subtype was determined by microsatellite analysis.[8,9] In brief, heterodisomy for at least one locus was regarded as indicative of TR- or GC-mediated UPD(14)pat (TR/GC subtype), whereas isodisomy for all the informative microsatellite loci was interpreted as indicative of MR- or PE-mediated UPD(14)pat (MR/PE subtype) (for details, see Supplementary Figure S1). Here, while heterodisomy and isodisomy for a pericentromeric region in the TR/GC subtype imply a disomic sperm generation through MI

Table 1 Summary of patients examined in this study

Patient	*Genetic cause*	*UPD(14)pat subtype*	*Maternal age at childbirth (years)*	*Paternal age at childbirth (years)*	*Remark*	*Reference*
1	UPD(14)pat	TR/GC [MI]	31	35		5
2	UPD(14)pat	TR/GC [MI]	28	29		5
3	UPD(14)pat	TR/GC [MI]	29	38		This report
4	UPD(14)pat	TR/GC [MI]	36	41		5
5	UPD(14)pat	TR/GC [M2]	30	30		This report
6	UPD(14)pat	MR/PE	42	Unknown		4,5
7	UPD(14)pat	MR/PE	31	28		5
8	UPD(14)pat	MR/PE	32	33		5
9	UPD(14)pat	MR/PE	26	35		5
10	UPD(14)pat	MR/PE	38	38		This report
11	UPD(14)pat	MR/PE	26	32		This report
12	UPD(14)pat	MR/PE	41	36		This report
13	UPD(14)pat	MR/PE	30	28		This report
14	UPD(14)pat	MR/PE	39	34		This report
15	UPD(14)pat	MR/PE	42	37	Born after IVF-ET	5
16	UPD(14)pat	MR/PE	36	36		4,5
17	UPD(14)pat-seg.	PE	27	24	Segmental isodisomy	4,5
18	Microdeletion		31	34		2
19	Microdeletion		33	36		2
20	Microdeletion		28	27		2
21	Microdeletion		27	37	IG-DMR alone	3
22	Microdeletion		25	25	*MEG3*-DMR alone	3
23	Epimutation		35	36		2
24	Epimutation		28	26		2
25	Epimutation		27	30		2
26	Epimutation		33	33		This report

Abbreviation: IVF-ET, *in vivo* fertilization-embryo transfer using parental gametes.
The microdeletions in patients 18–22 are different in size.

and M2 non-disjunction respectively,[9] such discrimination between M1 and M2 non-disjunctions is impossible for the development of a nullisomic oocyte. Furthermore, it is usually impossible to discriminate between TR and GC, although the presence of trisomic cells is specific to TR. Similarly, it is also usually impossible to discriminate between MR and PE, although identification of segmental isodisomy or mosaicism is unique to PE (PE subtype).

Analysis of parental ages

We examined parental ages at childbirth in patients of different underlying causes and different UPD(14)pat subtypes. Statistical significance of the relative frequency was examined by the Fisher's exact probability test, and that of the median age by the Mann–Whitney's *U*-test. $P<0.05$ was considered significant.

RESULTS

Analysis of underlying causes in patients with UPD(14)pat-like phenotype

For the eight new sporadic patients, methylation analysis invariably revealed hypermethylation of both DMRs, and microsatellite analysis showed UPD(14)pat in seven patients and biparentally inherited homologs of chromosome 14 in the remaining one patient (patient 26). FISH analysis for patient 26 identified two signals for the two DMRs, and subsequently performed array CGH analysis showed no evidence for genomic rearrangements (Supplementary Figure S2). Thus, patient 26 was assessed to have an epimutation affecting the two DMRs. Furthermore, the results of array CGH analysis confirmed the presence of microdeletions in patients 18–21 and the absence of a discernible microdeletion in patients 23–25 (Supplementary Figure S2) (array CGH analysis was not performed in patient 22 with a 4303-bp microdeletion[3] because of the lack of DNA sample available). Thus, together with our previous data, all the 26 patients with UPD(14)pat-like phenotype had genetic alteration involving the imprinted region on chromosome14q32.2.

Consequently, the 26 patients with UPD(14)pat-like phenotype were classified as follows: (1) 16 sporadic patients with full UPD(14)pat and 1 sporadic patient with segmental UPD(14)pat (UPD(14)pat group); (2) the proband of the sibling cases and two sporadic patients with different patterns of microdeletions involving the two DMRs, one sporadic patient with a microdeletion involving the IG-DMR alone in whom the *MEG3*-DMR was epimutated, and one patient with a microdeletion involving the *MEG3*-DMR alone (deletion group); and (3) four patients with epimutations (hypermethylations) of both DMRs (epimutation group) (Figure 1 and Table 1).

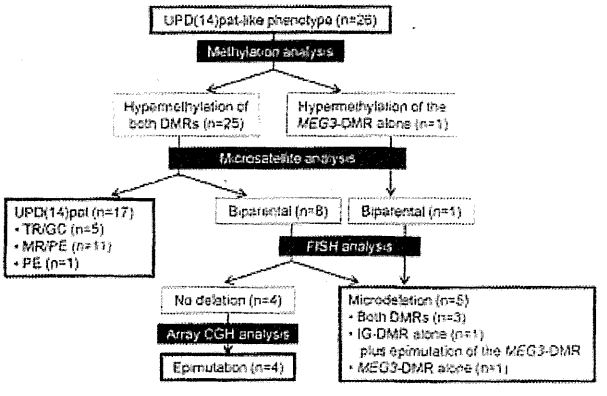

Figure 1 Classification of 26 patients with UPD(14)pat-like phenotype.

Analysis of subtypes in patients with UPD(14)pat

Heterozygosity for at least one locus indicative of TR/GC subtype was identified in five patients (patients 1–5), and the disomic pattern of pericentromeric region indicated M1 non-disjunction in patients 1–4 and M2 non-disjunction in patient 5. Full isodisomy consistent with MR/PE subtype was detected in 11 patients (patients 6–16), and segmental isodisomy unique to PE subtype was revealed in 1 patient (patient 17) (Table 1, Figure 1, and Supplementary Figure S3).

Analysis of parental ages

The distribution of parental ages at childbirth is shown in Figure 2. The advanced maternal age at childbirth (≥35 years) was predominantly observed in the MR/PE subtype of UPD(14)pat. Furthermore, while the relative frequency of aged mothers (≥35 years) did not show a significant difference between the MR/PE subtype of UPD(14)pat (6/11) and (i) other subtypes of UPD(14)pat (1/6) (P=0.159), (ii) deletion group (0/5) (P=0.057), and (iii) epimutation group (1/4) (P=0.338), it was significantly different between the MR/PE subtype and the sum of other subtypes of UPD(14)pat, deletion group, and epimutation group (2/15) (P=0.034). Similarly, while the median maternal age did not show a significant difference between the MR/PE subtype of UPD(14)pat (36 years) *vs* (i) other subtypes of UPD(14)pat (29.5 years) (P=0.118), (ii) deletion type (28 years) (P=0.088), and (iii) epimutation type (30.5 years) (P=0.295), it was significantly different between the MR/PE subtype of UPD(14)pat and the sum of other subtypes of UPD(14)pat, deletion group, and epimutation group (29 years) (P=0.045).

The paternal ages were similar irrespective of the genetic causes and the UPD(14)pat subtypes. In addition, the median paternal age was comparable between the TR/GC subtype of UPD(14)pat that postulates the production of a disomic sperm (35.0 years) and the sum of other subtypes of UPD(14)pat, deletion group, and epimutation group that assumes the production of a normal sperm (33.5 years) (P=0.322).

DISCUSSION

This study revealed that the UPD(14)pat-like phenotype was caused by UPD(14)pat in 65.4% of patients, by microdeletions in 19.2% of patients, and by epimutations in 15.4% of patients. Although the relative frequency of underlying genetic factors for the development of UPD(14)pat-like phenotype has been reported previously,[10] most data are derived from our previous publications. Thus, the present results are regarded as the updated and extended data on the relative frequency. For the relative frequency, it is notable that 25 of the 26 patients were confirmed to have normal karyotype, although chromosome analysis was not performed in patient 6. Thus, while Robertsonian translocations involving chromosome 14 is known to be a

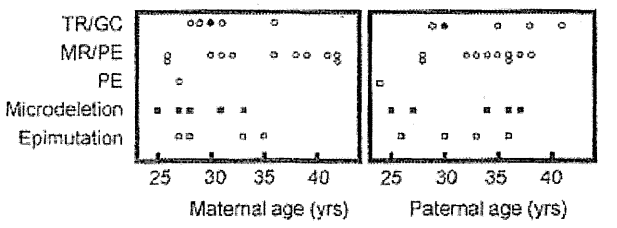

Figure 2 The distribution of parental ages at childbirth according to the underlying genetic causes for the development of UPD(14)pat-like phenotype and UPD(14)pat subtypes. Of the five plots for the TR/GC subtype, open and black circles indicate the TR/GC subtype due to non-disjunction at paternal M1 and M2, respectively.

predisposing factor for the occurrence of UPD(14)pat,[11–16] such a possible chromosomal effect has been excluded in nearly all patients examined in this study.

The relative frequency of underlying causes has also been reported in other imprinting disorders.[8,17–19] The data are summarized in Table 2 (a similar summary has also been reported recently by Hoffmann *et al*).[10] In particular, the results in patients with normal karyotype are available in Prader–Willi syndrome (PWS).[8] Furthermore, PWS is also known to be caused by UPD, microdeletions, and epimutations affecting a single imprinting region,[8,19] although Silver–Russell syndrome and Beckwith–Wiedemann syndrome (BWS) can result from perturbation of at least two imprinted regions,[17,18] and BWS and Angelman syndrome can occur as a single gene disorder.[17,19] Thus, it is notable that the relative frequency of underlying causes is quite different between patients with UPD(14)pat-like phenotype and those with PWS.[8,19] This would primarily be due to the presence of low copy repeats flanking the imprinted region on chromosome 15, because chromosomal deletions are prone to occur in regions harboring such repeat sequences.[20] Indeed, two types of microdeletions mediated by such low copy repeats account for a vast majority of microdeletions in patients with PWS,[21] whereas the microdeletions identified in patients with UPD(14)pat-like phenotype are different to each other. This would explain why microdeletions are less frequent and UPD and epimutations are more frequent in patients with UPD(14)pat-like phenotype than in those with PWS.

Advanced maternal age at childbirth was predominantly observed in the MR/PE subtype. This may imply the relevance of advanced maternal age to the development of MR-mediated UPD(14)pat, because the generation of nullisomic oocytes through M1 non-disjunction is a maternal age-dependent phenomenon.[22] Although no paternal age effect was observed, this is consistent with the previous data indicating no association of advanced paternal age with a meiotic error.[23] For the maternal age effect, however, several matters should be pointed out: (1) the number of analyzed patients is small, although it is very difficult to collect a large number of patients in this extremely rare disorder; (2) of the MR/PE subtype, the advanced maternal age is a risk factor for the generation of MR-mediated UPD(14)pat, but not for the development of PE-mediated UPD(14)pat; (3) it is impossible to discriminate between maternal age-dependent M1 non-disjunction and maternal age-independent M2 non-disjunction in the MR and GC subtypes (however, GC must be extremely rare, because it requires the concomitant occurrence of a nullisomic oocyte and a disomic sperm); (4) of the TR/GC subtype, the advanced maternal age is a risk factor for the generation of GC-mediated UPD(14)pat, but not for the development of TR-mediated UPD(14)pat; and (5) if a cryptic recombination(s) might remain undetected in some patients with apparently full isodisomy, this argues that such patients actually have TR- or GC-mediated UPD(14)pat rather than MR- or PE-mediated UPD(14)pat. Thus, further studies are required to examine the maternal age effect on the generation of MR-mediated UPD(14)pat. In addition, while a relationship is unlikely to exist between advanced maternal age and microdeletions and epimutations, this notion would also await further investigations.

Such a maternal age effect is also expected in the TR/GC subtype maternal UPDs after M1 non-disjunction, because the generation of disomic oocytes through M1 non-disjunction is also a maternal age-dependent phenomenon.[7] Indeed, such a maternal age effect has been shown for PWS patients with normal karyotype; the maternal age at childbirth was significantly higher in patients with heterodisomy for a very pericentromeric region indicative of TR/GC subtype UPD(15)mat after M1 non-disjunction than in those with other genetic causes.[8,9] For various chromosomes other than chromosome 15, furthermore, since maternal age at childbirth is higher in patients with maternal heterodisomy than in those with maternal isodisomy,[24] this would also argue for maternal age effect on the development of maternal UPDs. However, in the previous studies on maternal UPDs other than UPD(15)mat, the available data are quite insufficient to assess the maternal age effect. For example, although a relatively large number of patients with UPD(14)mat phenotype have been reported in the literature (reviewed in reference Hoffmann *et al*),[10] we could identify only six UPD(14)mat patients with normal karyotype in whom maternal age at childbirth was documented and microsatellite analysis was performed.[25–30] Furthermore, the microsatellite data are insufficient to identify the subtype of UPD(14)mat and to distinguish between M1 and M2 non-disjunction in the TR/GC subtype. Thus, while the maternal age at childbirth may be advanced in five patients with apparently TR/GC-mediated UPD(14)mat (27, 35, 37, 41, and 44 years)[25–27,29,30] (the maternal age at childbirth in the remaining one

Table 2 Relative frequency of genetic mechanisms in imprinting disorders

	UPD(14)pat-like phenotype	*BWS*	*SRS*	*AS*	*PWS*
Uniparental disomy	65.4%	16%	10%	3–5%	25% (25%)
	UPD(14)pat	UPD(11)pat (mosaic)	UPD(7)mat	UPD(15)pat	UPD(15)mat
Cryptic deletion	19.2%	Rare	—	70%	70% (72%)
Cryptic duplication	—	—	Rare	—	—
Epimutation					
Hypermethylation	15.4%	9%	—	—	2–5% (2%)
Affected DMR	IG-DMR/*MEG3*-DMR	*H19*-DMR	—	—	*SNRPN*-DMR
Hypomethylation	—	44%	>38%	2–5%	—
Affected DMR		KvDMR1	*H19*-DMR	*SNRPN*-DMR	
Gene mutation	—	5%	—	10–15%	—
Mutated gene		*CDKN1C*		*UBE3A*	
Unknown		25%	>40%	10%	
Reference	This study	17	18	19	8, 19

Abbreviations: AS, Angelman syndrome; BWS, Beckwith–Wiedemann syndrome; PWS, Prader–Willi syndrome; SRS, Silver–Russell syndrome.
Patients with abnormal karyotypes are included in BWS and AS, and not included in SRS. In PWS, the data including patients with abnormal karyotypes are shown, and those from patients with normal karyotype alone are depicted in parentheses.

patient with apparently MR/PE-mediated UPD(14)mat is 40 years),[28] the notion of a maternal age effect awaits further investigations for UPD(14)mat.

Finally, it appears to be worth pointing out that methylation analysis invariably revealed hypermethylated DMR(s) in all the 26 patients who were initially ascertained because of bell-shaped thorax with coat-hanger appearance of the ribs. This indicates that methylation analysis of the DMRs can be utilized for a screening of this condition, and that the constellation of clinical features in the UPD(14)pat-like phenotype, especially the bell-shaped thorax with coat-hanger appearance of the ribs, is highly unique to patients with UPD(14)pat-like phenotype.

In summary, this study confirms the relative frequency of underlying genetic causes for the UPD(14)pat phenotype and reveals the relative frequency of UPD(14)pat subtypes. Furthermore, the results emphasize the difference in the relative frequency of underlying genetic causes among imprinted disorders, and may support a possible maternal age effect on the generation of the nullisomic oocyte mediated UPD(14)pat. Further studies will permit a more precise assessment on these matters.

CONFLICT OF INTEREST

The authors declare no conflict of interest.

ACKNOWLEDGEMENTS

We thank Drs Kenji Kurosawa, Michiko Hayashidani, Toshio Takeuchi, Shinya Tanaka, Mika Noguch, Kouji Masumoto, Takeshi Utsunomiya, Yumiko Komatsu, Hirofumi Ohashi, Maureen J O'Sullivan, Andrew J Green, Yoshiyuki Watabe, Tsuyako Iwai, Hitoshi Kawato, Miho Torikai, Akiko Yamamoto, Nobuhiro Suzumori, Makoto Kuwajima, Hiroshi Yoshihashi, Yoriko Watanabe, and Jin Nishimura for material sampling and phenotype assessment. This work was supported by Grants for Research on Intractable Diseases (H22-161) and for Health Research on Children, Youth and Families (H21-005) from the Ministry of Health, Labor and Welfare, by Grants-in-Aid for Scientific Research (A) (22249010) and (B) (21028026) from the Japan Society for the Promotion of Science (JSPS), by Grants from Takeda Science Foundation and from Kanehara Foundation, and by the Grant for National Center for Child Health and Development (23A-1).

1 da Rocha ST, Edwards CA, Ito M, Ogata T, Ferguson-Smith AC: Genomic imprinting at the mammalian Dlk1-Dio3 domain. *Trends Genet* 2008; **24**: 306–316.
2 Kagami M, Sekita Y, Nishimura G *et al*: Deletions and epimutations affecting the human 14q32.2 imprinted region in individuals with paternal and maternal upd(14)-like phenotypes. *Nat Genet* 2008; **40**: 237–242.
3 Kagami M, O'Sullivan MJ, Green AJ *et al*: The IG-DMR and the MEG3-DMR at human chromosome 14q32.2: hierarchical interaction and distinct functional properties as imprinting control centers. *PLoS Genet* 2010; **6**: e1000992.
4 Kagami M, Nishimura G, Okuyama T *et al*: Segmental and full paternal isodisomy for chromosome 14 in three patients: narrowing the critical region and implication for the clinical features. *Am J Med Genet A* 2005; **138A**: 127–132.
5 Kagami M, Yamazawa K, Matsubara K, Matsuo N, Ogata T: Placentomegaly in paternal uniparental disomy for human chromosome 14. *Placenta* 2008; **29**: 760–761.
6 Shaffer LG, Agan N, Goldberg JD, Ledbetter DH, Longshore JW, Cassidy SB: American College of Medical Genetics statement of diagnostic testing for uniparental disomy. *Genet Med* 2001; **3**: 206–211.
7 Jones KT: Meiosis in oocytes: predisposition to aneuploidy and its increased incidence with age. *Hum Reprod Update* 2008; **14**: 143–158.
8 Matsubara K, Murakami N, Nagai T, Ogata T: Maternal age effect on the development of Prader-Willi syndrome resulting from upd(15)mat through meiosis 1 errors. *J Hum Genet* 2011; **56**: 566–571.
9 Robinson WP, Christian SL, Kuchinka BD *et al*: Somatic segregation errors predominantly contribute to the gain or loss of a paternal chromosome leading to uniparental disomy for chromosome 15. *Clin Genet* 2000; **57**: 349–358.
10 Hoffmann K, Heller R: Uniparental disomies 7 and 14. *Best Pract Res Clin Endocrinol Metab* 2011; **25**: 77–100.
11 Wang JC, Passage MB, Yen PH, Shapiro LJ, Mohandas TK: Uniparental heterodisomy for chromosome 14 in a phenotypically abnormal familial balanced 13/14 Robertsonian translocation carrier. *Am J Hum Genet* 1991; **48**: 1069–1074.
12 Papenhausen PR, Mueller OT, Johnson VP, Sutcliffe M, Diamond TM, Kousseff BG: Uniparental isodisomy of chromosome 14 in two cases: an abnormal child and a normal adult. *Am J Med Genet* 1995; **59**: 271–275.
13 Cotter PD, Kaffe S, McCurdy LD, Jhaveri M, Willner JP, Hirschhorn K: Paternal uniparental disomy for chromosome 14: a case report and review. *Am J Med Genet* 1997; **70**: 74–79.
14 Yano S, Li L, Owen S, Wu S, Tran T: A further delineation of the paternal uniparental disomy (UPD14): the fifth reported liveborn case. *Am J Hum Genet* 2001; **69** (Suppl): A739.
15 Kurosawa K, Sasaki H, Sato Y *et al*: Paternal UPD14 is responsible for a distinctive malformation complex. *Am J Med Genet A* 2002; **110**: 268–272.
16 McGowan KD, Weiser JJ, Horwitz J *et al*: The importance of investigating for uniparental disomy in prenatally identified balanced acrocentric rearrangements. *Prenat Diagn* 2002; **22**: 141–143.
17 Sasaki K, Soejima H, Higashimoto K *et al*: Japanese and North American/European patients with Beckwith-Wiedemann syndrome have different frequencies of some epigenetic and genetic alterations. *Eur J Hum Genet* 2007; **15**: 1205–1210.
18 Eggermann T: Epigenetic regulation of growth: lessons from Silver-Russell syndrome. *Endocr Dev* 2009; **14**: 10–19.
19 Gurrieri F, Accadia M: Genetic imprinting: the paradigm of Prader-Willi and Angelman syndromes. *Endocr Dev* 2009; **14**: 20–28.
20 Pujana MA, Nadal M, Guitart M, Armengol L, Gratacos M, Estivill X: Human chromosome 15q11-q14 regions of rearrangements contain clusters of LCR15 duplicons. *Eur J Hum Genet* 2002; **10**: 26–35.
21 Varela MC, Kok F, Setian N, Kim CA, Koiffmann CP: Impact of molecular mechanisms, including deletion size, on Prader-Willi syndrome phenotype: study of 75 patients. *Clin Genet* 2005; **67**: 47–52.
22 Pellestor F, Andreo B, Anahory T, Hamamah S: The occurrence of aneuploidy in human: lessons from the cytogenetic studies of human oocytes. *Eur J Med Genet* 2006; **49**: 103–116.
23 Sloter E, Nath J, Eskenazi B, Wyrobek AJ: Effects of male age on the frequencies of germinal and heritable chromosomal abnormalities in humans and rodents. *Fertil Steril* 2004; **81**: 925–943.
24 Kotzot D: Advanced parental age in maternal uniparental disomy (UPD): implications for the mechanism of formation. *Eur J Hum Genet* 2004; **12**: 343–346.
25 Fokstuen S, Ginsburg C, Zachmann M, Schinzel A: Maternal uniparental disomy 14 as a cause of intrauterine growth retardation and early onset of puberty. *J Pediatr* 1999; **134**: 689–695.
26 Hordijk R, Wierenga H, Scheffer H, Leegte B, Hofstra RM, Stolte-Dijkstra I: Maternal uniparental disomy for chromosome 14 in a boy with a normal karyotype. *J Med Genet* 1999; **36**: 782–785.
27 Sanlaville D, Aubry MC, Dumez Y *et al*: Maternal uniparental heterodisomy of chromosome 14: chromosomal mechanism and clinical follow up. *J Med Genet* 2000; **37**: 525–528.
28 Towner DR, Shaffer LG, Yang SP, Walgenbach DD: Confined placental mosaicism for trisomy 14 and maternal uniparental disomy in association with elevated second trimester maternal serum human chorionic gonadotrophin and third trimester fetal growth restriction. *Prenat Diagn* 2001; **21**: 395–398.
29 Aretz S, Raff R, Woelfle J *et al*: Maternal uniparental disomy 14 in a 15-year-old boy with normal karyotype and no evidence of precocious puberty. *Am J Med Genet A* 2005; **135**: 336–338.
30 Mitter D, Buiting K, von Eggeling F *et al*: Is there a higher incidence of maternal uniparental disomy 14 [upd(14)mat]? Detection of 10 new patients by methylation-specific PCR. *Am J Med Genet A* 2006; **140**: 2039–2049.

Supplementary Information accompanies the paper on European Journal of Human Genetics website (http://www.nature.com/ejhg)